AD-A157 432 SUBMILLIMETER QUANTUM ELECTRONICS(U) MASSACHUSETTS INST 1/1
OF TECH LEXINGTON LINCOLN LAB P E TANNENWALD 25 APR 85
ARO-19626.9-PH F19628-80-C-0002

UNCLASSIFIED F/G 9/3 NL

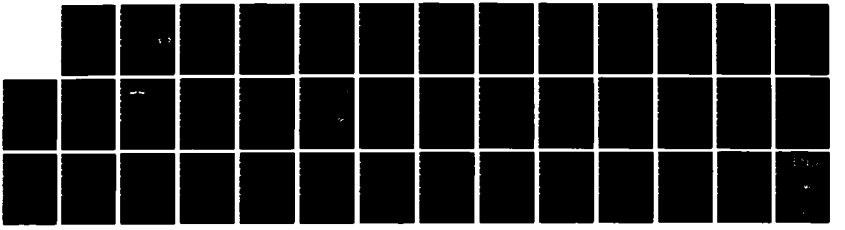

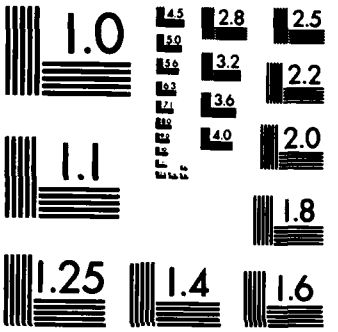

MICROCOPY RESOLUTION TEST CHART
NATIONAL BUREAU OF STANDARDS-1963-A

AD-A157 432

DTIC FILE COPY

UNCLASSIFIED
SECURITY CLASSIFICATION OF THIS PAGE (When Data Entered)

MASTER COPY - FOR REPRODUCTION PURPOSES

(2)

REPORT DOCUMENTATION PAGE

READ INSTRUCTIONS BEFORE COMPLETING FORM

1. REPORT NUMBER: ARO 19626.9-PH	2. GOVT ACCESSION NO.: N/A
3. RECIPIENT'S CATALOG NUMBER: N/A	
4. TITLE (and Subtitle): Submillimeter Quantum Electronics	5. TYPE OF REPORT & PERIOD COVERED: Final Report, 1 July 1982 - 31 March 1985
	6. PERFORMING ORG. REPORT NUMBER
7. AUTHOR(s): P. E. Tannenwald	8. CONTRACT OR GRANT NUMBER(s): MIPR ARO 129-85; F19628-80-C-0002; F19628-85-C-0002
9. PERFORMING ORGANIZATION NAME AND ADDRESS: Lincoln Laboratory, M.I.T.	10. PROGRAM ELEMENT, PROJECT, TASK AREA & WORK UNIT NUMBERS
11. CONTROLLING OFFICE NAME AND ADDRESS: U. S. Army Research Office, Post Office Box 12211, Research Triangle Park, NC 27709	12. REPORT DATE: 25 April 1985
	13. NUMBER OF PAGES: 5 pages + 6 Appendices
14. MONITORING AGENCY NAME & ADDRESS (if different from Controlling Office)	15. SECURITY CLASS. (of this report): Unclassified
	15a. DECLASSIFICATION/DOWNGRADING SCHEDULE

16. DISTRIBUTION STATEMENT (of this Report)

Approved for public release; distribution unlimited.

DTIC ELECTE AUG 06 1985 S E D

17. DISTRIBUTION STATEMENT (of the abstract entered in Block 20, if different from Report)

NA

18. SUPPLEMENTARY NOTES

The view, opinions, and/or findings contained in this report are those of the author(s) and should not be construed as an official Department of the Army position, policy, or decision, unless so designated by other documentation.

19. KEY WORDS (Continue on reverse side if necessary and identify by block number)

Resonant Tunneling	Quantum Well Oscillations	Submillimeter LO
GaAs/GaAlAs MBE	Persistent Photoconductivity	Submillimeter Astronomy
Quantum Wells	Mm & Submm Heterodyning	Submillimeter Radiometer/Receiver

20. ABSTRACT (Continue on reverse side if necessary and identify by block number)

Tunneling phenomena have been explored in quantum wells consisting of GaAs/GaAlAs heterostructure layers that were grown by molecular beam epitaxy. Devices such as detectors and mixers have been fabricated from these quantum wells that showed characteristic tunneling response from DC to 2.5 THz. In addition, the negative differential resistance that was observed was used to demonstrate microwave oscillations up to 20 GHz, both at low temperatures and at room temperature. A variety of other submillimeter

DD FORM 1 JAN 73 1473 EDITION OF 1 NOV 65 IS OBSOLETE

UNCLASSIFIED
SECURITY CLASSIFICATION OF THIS PAGE (When Data Entered)

experiments are described in the reprints included in the appendices: heterodyning from millimeter wave to optical frequencies using GaAs MESFETs above f_T, heterodyne radiometry measurements of the 557 GHz water vapor rotational line, development of a submillimeter radiometer using a solid-state local oscillator, and submillimeter astronomical observations carried out at telescope field sites. Also mentioned are persistent photoconductivity observed in quantum wells and a low-IF submillimeter heterodyne receiver to be used in electromagnetic scattering experiments.

Accession For	
NTIS GRA&I	X
DTIC TAB	☐
Unannounced	☐
Justification	
By	
Distribution/	
Availability Codes	
Dist	Avail and/or Special
A-1	

DTIC COPY INSPECTED 3

ARO 19626.9-PH

SUBMILLIMETER QUANTUM ELECTRONICS

FINAL REPORT

P. E. TANNENWALD

25 APRIL 1985

U. S. ARMY RESEARCH OFFICE

GRANT NUMBER 19626-PH

LINCOLN LABORATORY

MASSACHUSETTS INSTITUTE OF TECHNOLOGY

APPROVED FOR PUBLIC RELEASE;

DISTRIBUTION UNLIMITED

85 7 25 072

TABLE OF CONTENTS

I. INTRODUCTION

During the last few years the technology in the near-millimeter and submillimeter regions of the spectrum has been developing rapidly so that significant applications have been realized. For example, tunable high-resolution spectroscopy using lasers, radic astronomical observations, plasma diagnostics and submillimeter radar modeling are being actively pursued. Important projects can now be realistically planned for high-altitude aircraft and satellite-based aeronomy, astronomy, and perhaps surveillance. Desirable components that are yet to be perfected are imaging array detectors and solid state sources; the two may well be related because any solid state oscillators in the submillimeter are likely to be weak and will require an array operating as a combiner/radiator.

The availability and refinement of molecular beam epitaxy (MBE) has had a profound influence on electronic device fabrication technology. Virtually every semiconductor device is being improved through this technique, and equally important, a variety of new structures, physical phenomena and devices can now be conceived and investigated.

At Lincoln Laboratory we have placed our primary effort in the recent ARO program on the fabrication of GaAs/GaAlAs heterostructures in order to study the physics of tunneling phenomena in such structures, to explore the negative differential resistivity, and to develop detectors, mixers and oscillators at high frequencies. The results so far have been exceedingly encouraging, so that we are planning to improve the present devices as well as propose the investigation of a variety of new phenomena involving electron oscillations in coupled quantum wells, multiple-well effects, and tunneling devices in the form of transistors, detectors and lasers.

II. RESULTS

Progress during the contract period has been reported in the semiannual progress reports to ARO. Below are listed significant highlights, details of which appear in the reprints and preprints that are appended to this proposal, plus the most recent progress. In most cases the work received additional support from other sponsors.

1. Resonant Tunneling Through Quantum Wells - Resonant tunneling has been observed through a single quantum well of GaAs grown by MBE between two barriers of GaAlAs (double barrier structure). The current singularity and negative resistance region are dramatically improved over previous results. Detection and mixing experiments carried out at frequencies as high as 2.5 THz show the intrinsic response time to be less than 10^{-13} sec. Resonant tunneling features are visible in the conductance-voltage curve at room temperature and become quite pronounced in the I-V curves at low temperature. (See Appendix I for details.)

2. Quantum Well Oscillations - Oscillations have been observed for the first time from a quantum well resonant tunneling structure. For pure material in the wells, the current density is high enough to provide sufficient gain and adequate impedance match to the resonant circuit so that the devices oscillate readily in the negative resistance region. Oscillator output power of 5 μW and frequencies up to 18 GHz have been obtained with a DC to RF efficiency of 2.4% at temperatures as high as 200 K. (See Appendix II for details.) Very recently, oscillations have been obtained at room temperature at 19.7 GHz, but the results have not yet been prepared for publication.

3. Persistent Photoconductivity in Quantum Well Resonators - Several photoconductive effects with characteristic time constants between nanoseconds and minutes have been observed in double-barrier tunneling structures. In the persistent (long time constant) photoconductivity experiments, as the number of photons increases, the resonant current peak in the I-V curves increases and shifts to lower voltages. This is explained by modifications to the conduction band of the double-barrier structure due to positive charges in the barrier. These positive charges arise from ionization of DX centers which are known to exist in Si-doped AlGaAs. Calculated I-V curves agree with measured ones, and the derived DX center density agrees with estimates from material growth parameters. (This subject matter is being prepared for publication.) The high-speed photoconductive mixing effects were observed by means of laser mode beating. They are under further investigation to establish the limiting process, whose time constant is likely to be of the order of 100 fs. Tunneling current calculations have been refined to include the effects of charge accumulation and depletion at the barrier interfaces, leading to a better fit to the experimental I-V curves. Controlling the depletion region outside the barrier by suitable doping can decrease the capacitance and thereby raise the cut-off frequency of tunneling devices toward their intrinsic limit.

4. Heterodyne Experiments from Millimeter Wave to Optical Frequencies Using GaAs MESFETs above f_T - Response of GaAs FETs in millimeter-wave and optical heterodyne experiments has been obtained at frequencies above the frequency of unity current gain, f_T. In the mixing of two visible lasers, beat frequencies as high as 300 GHz have been observed. These

high IFs were down-converted to microwave frequencies by radiatively coupling millimeter-wave local oscillators into the gate region. The results indicate that GaAs FETs can be used as sensitive and versatile detectors and mixers of millimeter-wave and optical radiation. As millimeter mixers, results have been obtained up to 350 GHz. (See Appendix III for further details.)

5. Solid-State Submillimeter Heterodyne Radiometer - We have developed a solid-state submillimeter-wave radiometer which we have used to measure the rotational temperature of the H_2O transition at 557 GHz ($1_{10} \leftarrow 1_{01}$) in a water vapor jet expanding into a high-vacuum chamber, repeating earlier measurements which used a laser or carcinotron local oscillator. (See, e.g., APPENDIX IV.) Key advances in this radiometer are its high sensitivity, stability, compactness and low operating power requirement. A 50 mW Varian InP Gunn diode (made available by Dr. Lothar Wandinger, U. S. Army Electronics R & D Command) oscillating at 92.6 GHz drove a frequency tripler and doubler in cascade. The doubler, operating in the harmonic mixer mode, served as local oscillator at 557 GHz for the heterodyne radiometer. The best noise temperature in the experiment was 6000 K (DSB), while at slightly different frequencies we could obtain less than 4500 K (DSB). The water vapor line could be traced out with 0.5 MHz resolultion (the sextupled jitter of the Gunn) and a S/N of > 20. A prominent self-reversal feature due to a warmer central core of the jet was observed. This demonstration experiment shows that a compact LO with low input power requirements could be developed for a satellite-based radiometer. NASA is proceeding with this concept for

submillimeter astronomy, and other space-based applications can be envisioned. A short publication is under preparation. (This project was carried out in collaboration with N. Erickson, Five College Radio Astronomy Observatory, U. Mass., Amherst.)

6. Low-IF Submillimeter Heterodyne Receiver - We have demonstrated the feasibility of heterodyne detection at low ($\approx$ 1 MHz) IF frequencies. Heterodyning is obtained in a corner cube mixer by using one far-IR laser as signal source and a second one, operating on the same laser line, as the LO. A crucial feature is a frequency tracking chain which ensures that the beat frequency between the two laser outputs, after a second conversion, remains stable to less than 50 kHz. The tracking system consists of a computer-coupled IF frequency counter and a frequency synthesizer that generates a correction frequency which is fed to a second mixer. The receiver will be used for electromagnetic scattering measurements in the far IR spectral region for an Army project.

7. Submillimeter Radiometer Field Measurements - As a result of earlier support by ARO, which led to the development of low-noise Schottky diode mixers in the submillimeter, we have collaborated with other groups in the application of sensitive radiometers to astronomical problems. During a third expedition to the Mauna Kea Observatory in Hawaii, the distribution of the $J = 6 \rightarrow 5$ transition of CO in Orion was measured for the first time, and several first detections were made of the same transition in other galactic sources. (See APPENDIX V for details.) The general techniques of carrying out submillimeter radio astronomical measurements are described in APPENDIX VI.

Resonant tunneling through quantum wells at frequencies up to 2.5 THz

T. C. L. G. Sollner, W. D. Goodhue, P. E. Tannenwald, C. D. Parker, and D. D. Peck
Lincoln Laboratory, Massachusetts Institute of Technology, Lexington, Massachusetts 02173

(Received 9 May 1983; accepted for publication 1 July 1983)

Resonant tunneling through a single quantum well of GaAs has been observed. The current singularity and negative resistance region are dramatically improved over previous results, and detecting and mixing have been carried out at frequencies as high as 2.5 THz. Resonant tunneling features are visible in the conductance-voltage curve at room temperature and become quite pronounced in the *I-V* curves at low temperature. The high-frequency results, measured with far IR lasers, prove that the charge transport is faster than about 10^{-13} s. It may now be possible to construct practical nonlinear devices using quantum wells at millimeter and submillimeter wavelengths.

PACS numbers: 73.40.Gk, 73.40.Lq

Quantum wells are the subject of considerable theoretical and experimental study. They consist of thin (< 100 Å) layers of material, usually a semiconductor confined between two layers of a different material with a larger band gap. In this way carriers are confined to the lower band-gap material. The most studied system uses molecular beam epitaxy (MBE) to fabricate GaAs wells adjacent to $Ga_{1-x}Al_xAs$ barriers. The properties of the wells are usually studied optically or characterized by their transport behavior. If the barriers are sufficiently thin, then carriers can tunnel through them, and it becomes possible to probe the quantum wells with carriers. We have studied resonant tunneling through a single quantum well of such a system.

In this letter we report the first observation of resonant tunneling at room temperature and a broad region of negative resistance which is already observable at 200 K. At 25 K we have observed the largest peak to valley ratio yet reported (6:1). By comparing high-frequency current response measurements with the observed dc characteristics we have established that response times are less than 10^{-13} s and are thus consistent with tunneling. In addition, we have carried out mixing experiments in these devices at various millimeter and submillimeter wavelengths down to 119 μm.

Tsu and Esaki[1] have shown that a large peak in the tunneling current should occur when the injected carriers have certain resonant energies. Figure 1 shows schematically how resonance occurs with applied dc bias. The electrons originate near the Fermi level to the left of the first barrier of height ΔE, tunnel into the well, and finally tunnel through the second barrier into unoccupied states. Resonance occurs when the electron wave function reflected at the first barrier is cancelled by the wave which leaks from the well in the same direction or, equivalently, when the energy of the injected carrier becomes approximately equal to the energy level of the electrons confined in the well.

Previous measurements of heterojunction quantum well structures have shown evidence of resonant tunneling. At low temperatures Chang *et al.*[2] have observed structure in the conductance (dI/dV) voltage curve, and occasionally negative resistance for a single quantum well in the $Ga_{1-x}Al_xAs$ system grown by MBE. Vojak *et al.*[3] have also observed negative resistance at 77 K in multilayer $Al_xGa_{1-x}As$ heterostructures grown by metalorganic chemical vapor deposition using a *p-n* junction for charge injection. These previous measurements, however, have shown only small regions of negative resistance, if any, and near unity peak to valley ratios. No resonant tunneling features were observed at room temperature. Also no measurements of response time were reported.

The structure, shown schematically in Fig. 1, was pre-

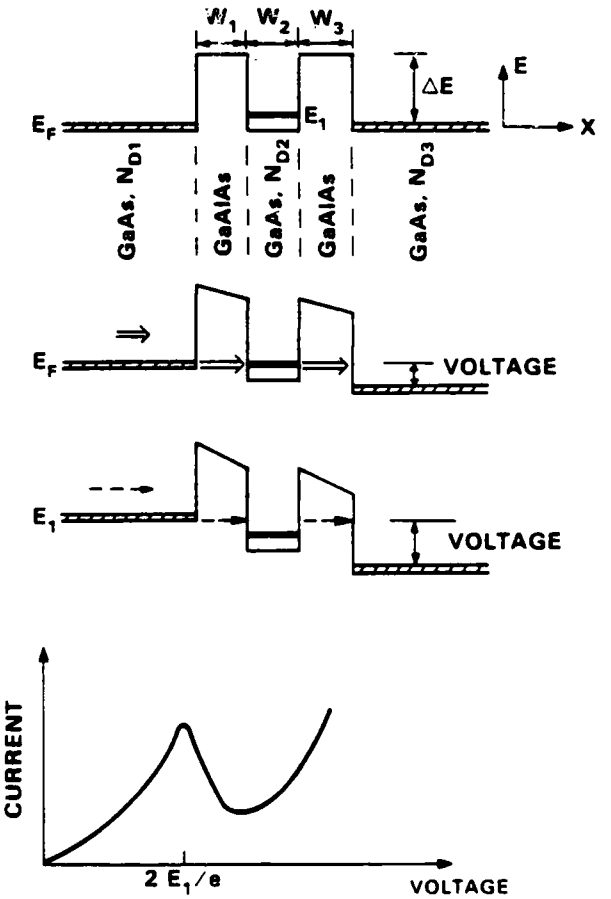

FIG. 1. Electron energy as a function of position in the quantum well structure. The parameters are $N_{D1} = N_{D3} = 10^{18}$ cm^{-3}, $N_{D2} = 10^{17}$ cm^{-3}, and $W_1 = W_2 = W_3 = 50$ Å. The doping level in the well center is an average value achieved by placing a layer of 10^{18} cm^{-3} material in the central 10% of the well. The energy level E_1 occurs above the bottom of the bulk conduction band because of confinement in the x direction. From the aluminum concentration ($x \simeq 25\%$–30%) we estimate $\Delta E = 0.23$ eV.

 0003-6951/83/180588-03$01.00 © 1983 American Institute of Physics

pared by molecular beam epitaxy on an n-type wafer of GaAs. The net donor concentration (Si) in the GaAs outside the barriers is 10^{18} cm^{-3}, and the GaAs well was doped to an average concentration of 10^{17} cm^{-3} by placing a layer of 10^{18} cm^{-3} material in the central 10% of the well. The resulting band bending within the well is negligible compared to kT. The top layer of GaAs is about 5000 Å thick. The barriers of $Ga_{0.75}Al_{0.25}As$ were not intentionally doped and are presumed to be semi-insulating owing to defect compensation. The substrate growth temperature was 680 °C and the flux ratio of As to Ga as measured from an ion gauge placed at the substrate growth position was 19:1. The Al concentration was measured by analysis of scanning transmission electron induced x rays from the barriers and from measurements of thicker films grown under similar conditions. Both methods gave $x = 25\%$–30%. The barrier and well dimensions of 50 Å were determined by transmission electron microscopy.

Arrays of mesas, 5 μm square, were etched into the completed wafer with Ohmic contacts top and bottom. The wafers were then diced into 10-mil square chips and mounted in a corner cube detector mount with a whisker contacting the mesas. The corner cube structure has been used routinely in our laboratory for mounting Schottky diodes to be used as detectors and mixers and is well characterized at submillimeter wavelengths.[4]

The observed dc current-voltage and conductance-voltage curves are shown in Fig. 2 for several temperatures. Notice that even at 300 K there are features in the conductance curve, and that a broad region of negative differential resistance exists at 200 K. At temperatures below 50 K the transmission peaks occur at an average voltage of 0.218 V. The peak to valley ratio is 6:1 on the positive side and 4.8:1 for negative voltages. The asymmetry may be due to slightly different barrier thicknesses, or heights, and may also involve interface states at the GaAs-GaAlAs interface.

Submillimeter measurements were made at 138 GHz, 761 GHz, and 2.5 THz with a carcinotron and far IR lasers, respectively. We measured the current response as a function of dc bias voltage. The calculated current responsivity $\mathcal{R}_i$ is given by

$$\mathcal{R}_i = \frac{\Delta I}{\Delta P_{\text{avail}}} = \frac{I'' Z_A}{(1 + Z_A/R_s)^2}\left(\frac{1}{\omega R_s C}\right)^2. \qquad (1)$$

This expression is obtained following Torrey and Whitmer,[5] but accounting for the mismatch between the antenna impedance Z_A of the corner cube and the device impedance in the limit $\omega R_s C \gg 1$ and $R_s \ll (dI_{dc}/dV)^{-1}$. Here, I'' is the second derivative of the dc I-V curve, C the device capacitance, ω the angular frequency, and R_s the series resistance. We have used $Z_A = 50\,\Omega$ from model measurements on the corner cube at 10 GHz. This value is uncertain by perhaps a factor of 2 because of the large scaling factor. The series resistance was calculated from the sum of the spreading resistance (2 Ω), resistance of the overgrown GaAs (4 Ω), and skin resistance of the chip (5.5 Ω). The capacitance is just the barrier capacitance of 290 fF as calculated from the device dimensions.

At all three frequencies the measured current response agrees with the calculated value within a few decibels. In Fig. 3, expanding on an approach used first by Small *et al.*,[6] we show the measured and calculated current response at 2.5 THz. Since the general shape of the two curves is the same, it follows that the I-V curve at 2.5 THz must be very similar to the dc I-V curve. In addition, the magnitude of the calculated current response agrees rather well with the measured curve considering the uncertainties in the parameters of Eq. (1). The somewhat greater discrepancy between measured and calculated values at large voltages may be due to quantum effects of photon assisted tunneling. The agreement is sufficient to show that the charge transport mechanism is at least as fast as the angular period of 2.5 THz, i.e., $\tau = 6 \times 10^{-14}$ s. Further verification has been obtained by mixing two sources near 140 GHz in the device, as well by the observation of far infrared laser mode beats at 434 and 119 μm. These first quantum well structures were not meant to compete with Schottky diodes as detectors. (The responsivity is smaller by over an order of magnitude.) But with dif-

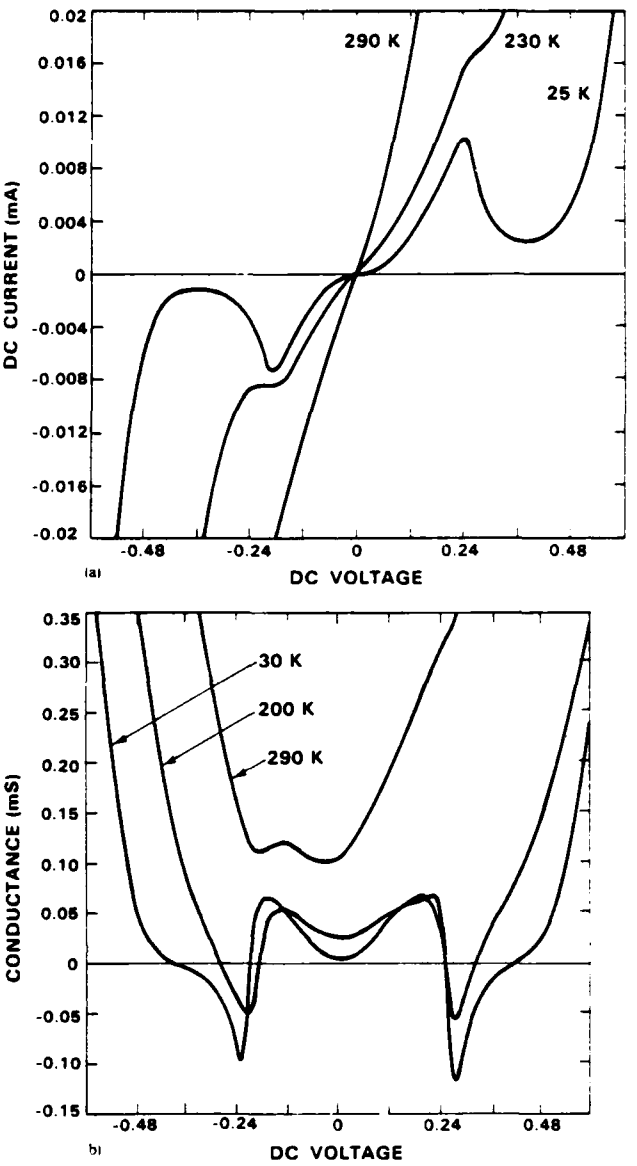

FIG. 2. (a) Current-voltage and (b) conductance (dI/dV)-voltage curves at three temperatures. Notice that resonant tunneling features can be seen even at room temperature.

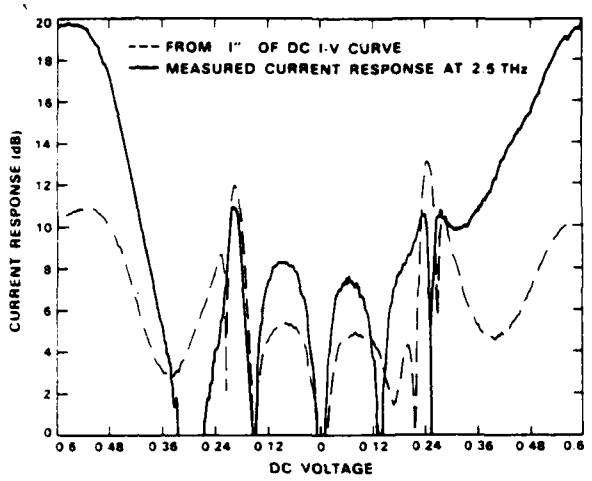

FIG. 3. Current response at 2.5 THz as a function of dc bias voltage. (Sample is at 25 K.) The dashed curve is calculated on the basis of the dc I-V curve. Zero decibels corresponds to 0.3 μA/W and 10 dB is 3 μA/W. The general agreement shows that the I-V curve at 2.5 THz is very similar to the dc curve, and thus the charge transport is fast.

ferent structure parameters and a reduction in capacitance, high-frequency sensitivity can probably be improved.

The time required for electrons to transit both barriers and the well can be estimated by assuming that tunneling times are approximately given by the uncertainly relation, $\tau \leqslant h/\Delta E$. From our estimate of the Al concentration ($x \simeq 25\%$–30%) in the barriers, and optical measurements of barrier heights,[7] $\Delta E \approx 0.23$ eV. The electrons outside the barrier region have a Fermi velocity of 5×10^7 cm/s, so we assume for simplicity that they move through the well region at the saturation velocity of about 10^7 cm/s. This yields a total transit time estimate of order 10^{-13} s. Other estimates of the tunneling time[8] reduce the total transit time estimate by about a factor of 2.

The tunneling current density of these devices is rather low for practical applications in view of the large capacitance ($RC = 3 \times 10^{-12}$ s). Chang *et al.*[2] have shown that a decrease of barrier width by a factor of 2 results in an increase in current density of two orders of magnitude. We will investigate the lower limits of barrier thickness in the future.

We have fabricated a second MBE wafer of nominally identical configuration to that of Fig. 1 and find very similar results. The quantum well thickness and the barrier heights seem to be reproducable within 10%–20%. Three devices randomly chosen from the same wafer were found to be virtually identical.

The existence of a large negative resistance at very high frequencies suggests applying these devices to millimeter and submillimeter amplifiers and oscillators by designing appropriate resonance circuits and matching the device to the resonator. Since these devices can be fabricated with planar technology, feedback and antenna elements could be placed very near the active area, reducing losses. Also, arrays of elements could be used in distributed circuits.

In conclusion, fabrication of high quality, reproducible, high speed resonant tunneling structures has been demonstrated. It now appears feasible to construct practical nonlinear solid state devices using quantum wells at millimeter and submillimeter wavelengths.

It is a pleasure to express our appreciation to the many people who helped in the fabrication of these devices, in particular A. R. Forte, G. D. Johnson, J. T. Kelliher, J. J. Lambert, I. H. Mroczkowski, and N. Usiak. B. J. Clifton kindly supplied the corner cube mounts. Also we benefited from discussions with A. R. Calawa, B. Lax, H. Le, and B. A. Vojak. Assistance from A. J. Garratt-Reed of the MIT Center for Materials Science and Engineering for scanning transmission electron microscope measurements is gratefully acknowledged. We especially thank H. R. Fetterman who participated in the initiation of the superlattice program at Lincoln Laboratory. This work was sponsored by the U.S. Army Research Office.

[1] R. Tsu and L. Esaki, Appl. Phys. Lett. **22**, 562 (1973).
[2] L. L. Chang, L. Esaki, and R. Tsu, Appl. Phys. Lett. **24**, 593 (1974).
[3] B. A. Vojak, S. W. Kirchoefer, H. Holonyak, Jr., R. D. Dupuis, P. D. Dapkus, and R. Chin, J. Appl. Phys. **50**, 5830 (1979).
[4] H. R. Fetterman, P. E. Tannenwald, B. J. Clifton, C. D. Parker, W. D. Fitzgerald, and N. R. Erickson, Appl. Phys. Lett. **33**, 151 (1978).
[5] H. C. Torrey and C. A. Whitmer, *Crystal Rectifiers* (McGraw-Hill, New York, 1948), p. 336.
[6] J. G. Small, G. M. Elchinger, A. Javan, A. Sanchez, F. J. Bachner, and D. L. Smythe, Appl. Phys. Lett. **24**, 275 (1974).
[7] R. Dingle, *Festkörper Probleme XV, Advances in Solid State Physics* (Pergamon, New York, 1975), pp. 21–48.
[8] M. Buttiker and R. Landauer, Phys. Rev. Lett. **49**, 1739 (1982).

APPENDIX II.

Quantum well oscillators

T. C. L. G. Sollner, P. E. Tannenwald, D. D. Peck, and W. D. Goodhue
Lincoln Laboratory, Massachusetts Institute of Technology, Lexington, Massachusetts 02173

(Received 17 August 1984; accepted for publication 25 September 1984)

Oscillations have been observed for the first time from double barrier resonant tunneling structures. By eliminating impurities from the wells, we have been able to increase the tunneling current density by a factor of nearly 100. With the attendant increase in gain and improved impedance match to the resonant circuit, the devices oscillated readily in the negative resistance region. Oscillator output power of 5 μW and frequencies up to 18 GHz have been achieved with a dc to rf efficiency of 2.4% at temperatures as high as 200 K. It is shown that higher frequencies and higher powers can be expected.

Negative differential resistance has been observed previously in double barrier resonant tunneling structures[1,2] (quantum well resonators), recently with large peak-to-valley ratios[2] (6 to 1) and fast charge transport[2] ($\tau < 10^{-13}$ s). The high impedance of those earlier devices prevented oscillations, but allowed observation of the negative differential resistance region since they could be stably biased by a lower impedance voltage source at all frequencies. Under the correct circuit conditions, microwave oscillations would be expected from quantum well resonators because of the high speed negative differential resistance. For oscillations to be observed it is necessary to terminate the negative differential impedance with a positive impedance of the same order.

In this letter we report the first observation of oscillations from a quantum well resonator. (The tunneling mechanism involved here is in contrast to the GaAs/GaAlAs heterojunction real-space transfer oscillator reported by Coleman *et al.*[3] to oscillate at 25 MHz.) Fabrication of much higher current density devices allowed the negative impedance to be more closely matched to coaxial component impedances. The maximum output power of 5 μW remained relatively constant up to temperatures of 200 K. The maximum

 0003-6951/84/241319-03$01.00 © 1984 American Institute of Physics

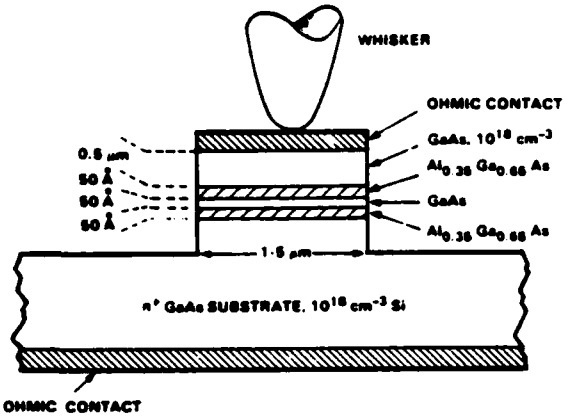

FIG. 1. Physical geometry of quantum well mesa in cross section. The higher band gaps of the two $Al_{0.35}Ga_{0.65}As$ layers act as partially reflecting mirrors to produce an electron Fabry–Perot etalon enclosing the thin GaAs quantum well.

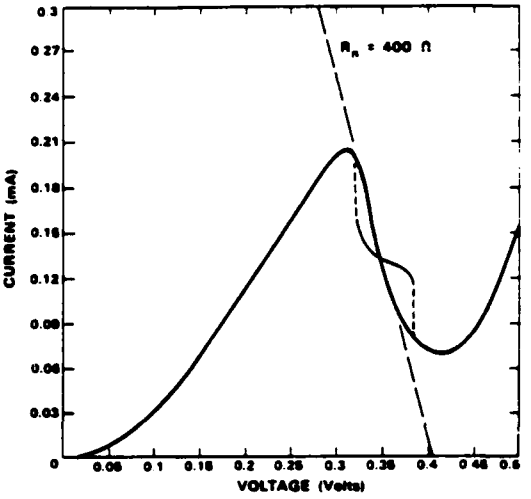

FIG. 2. Current-voltage characteristic for a quantum well resonator at 100 K. The dark line is the true curve for a stable device; the light line was measured when oscillating at 4 GHz. The difference is due to self-detection.

observed frequency of oscillation was 18 GHz. This was limited more by the coaxial circuits as described below than by the intrinsic time constants of the quantum well resonator. These results are consistent with the more indirect observation in Ref. 2 of rapid response times.

The mesa-isolated quantum well resonator, as fabricated, is shown in Fig. 1. A typical mesa diameter is 3 μm. The layered structure is grown on an n^+ substrate by molecular beam epitaxy. A thin layer of GaAs is sandwiched between two thin layers of $Ga_{0.7}Al_{0.3}As$. The addition of aluminum raises the band gap above that of GaAs so these regions act as partially transparent mirrors to electrons, the charge transport taking place by tunneling through the 50-Å-thick barriers. These two mirrors form a sort of electron Fabry–Perot resonator with peaks in the electron transmission (current) as a function of incident electron energy (voltage).

It is clear from the Fabry–Perot analogy that coherence of the electron wave function is required across the entire double barrier region. Any scattering which occurs in either the well or barriers will destroy this coherence, greatly reducing the probability of transmission through the double barrier region. In previously reported structures the well region contained approximately 10^{17} cm^{-3} donor atoms. By eliminating these impurities, so that the well was nominally undoped, the tunneling current density has been increased by a factor of 100.

It is possible to damp the oscillators of the devices with negative impedances of greater than a few hundred ohms by applying a broadband (0.1–18 GHz) 50-Ω termination. Figure 2 shows such an I-V curve of a device at 100 K traced out by a dc voltage source. The dark curve shows the true I-V curve of the quantum well resonator. The light curve was taken when the device was oscillating, under conditions described below, at 4 GHz. The shift is due to the current response from self-detection of the oscillations. This interpretation is confirmed by the fact that the sign of the current response is the same as the curvature of the I-V curve, becoming zero at the inflection point. The dashed lines indicate the discontinuous transition between stable and oscillating states.

A coaxial resonant cavity was used for these oscillators with the quantum well resonator at one end of the cavity, as shown schematically in Fig. 3. The minimum cavity length we could easily achieve resulted in a maximum fundamental oscillation frequency of 9 GHz. However, it was sometimes possible to observe oscillation in the higher modes so that frequencies up to 18 GHz were obtained. This was the maximum frequency for which the coaxial circuit components were well behaved.

The spectrum of a quantum well resonator oscillating at 8.2 GHz and at a temperature of 200 K is shown in Fig. 4. The bandwidth here is limited by the spectrum analyzer resolution, but in measurements at higher resolution the bandwidth was limited by mechanical stability of the cavity to about 10 kHz. The wings 40 dB below the peak, which extend out to a few MHz, are probably due to low-frequency noise mechanisms in the charge transport process.

The observed output in this case is 5 μW. The maximum available power from such negative resistance devices is given by[4]

$$P_{\max} = \frac{3}{16}\Delta V \Delta I, \tag{1}$$

where ΔV (ΔI) is the voltage (current) extent of the negative resistance. In this case the maximum available power is 17 μW. In view of the fact that no matching optimization has been attempted, this is reasonable agreement. The observed dc to rf efficiency is 2.4% and the maximum efficiency based

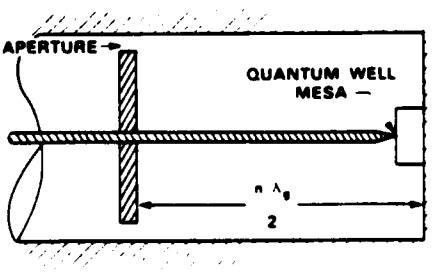

FIG. 3. Coaxial cavity used as resonant circuit for oscillating quantum well resonators.

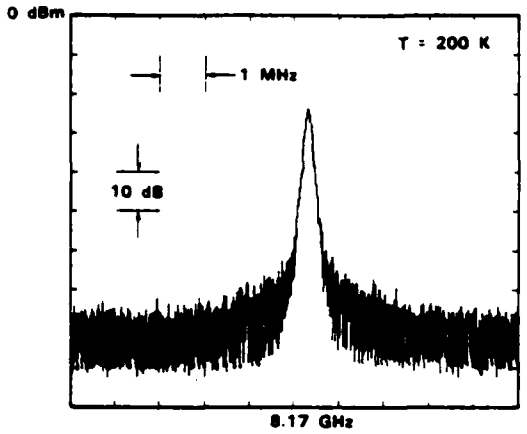

FIG. 4. Spectrum of oscillating quantum well resonator. The wings below − 60 dBm which extend to a few MHz are probably due to low frequency noise in the charge transport process.

on Eq. (1) would be about 8%. Past work on tunnel diodes[5] has achieved output powers higher than these due primarily to their higher current density and somewhat higher ΔV. (We discuss increasing the current density in quantum well devices below.)

The maximum oscillation frequency we have measured from this circuit is 18 GHz. The maximum oscillating frequency one could expect from a negative resistance device with fast charge transport is given by[6]

$$f_{max} = 1/2\pi C\sqrt{R_s R_n}, \tag{2}$$

where R_s is the series resistance, R_n is the negative differential resistance, and C is the capacitance. For the rather large area devices we are currently using, this frequency is 35 GHz. This can be raised in several ways. The current density has already been increased (hence decreasing R_n for a given C) by two orders of magnitude over earlier devices by reducing scattering. Our calculations show that another factor of 5 can be gained by a further reduction in scattering, and there is at least another factor of 10 to be gained by changing barrier thicknesses.

If impedance levels get too low because of the higher current density, either a smaller diameter or a series connected stack could be used. With these methods, oscillation frequencies of a few hundred gigahertz could be achieved. The output power would also be increased by increasing the current density.

Above-band-gap radiation generally increases the output power. Several photoconductive effects with characteristic time constants between nanoseconds and minutes have also been observed. These will be studied in more detail and reported in the future.

Quantum well resonators are promising as a source of high frequencies at low power. Although individually they are not particularly powerful, the very high volume power density (40 MW/cm^3) suggests that power combining techniques could greatly increase the total output. The powerful methods of molecular beam epitaxy and planar lithography could produce monolithic structures with integrated antennas, resulting in high power coherent arrays similar to phased laser diode arrays. Another possible use for quantum well resonators is as self-oscillating mixers, since they have already demonstrated the ability to mix at submillimeter wavelengths.[2] The possibility of using the negative resistance for amplification at high frequencies remains to be explored.

We are pleased to express our appreciation to those who helped fabricate these devices, especially J. J. Lambert, I. H. Mroczkowski, and N. Usiak. Useful discussions were had with A. R. Calawa, H. Q. Le, B. A. Vojak, and H. J. Zeiger. We would especially like to thank R. A. Kiel of AT&T Bell Laboratories for some helpful suggestions. This work was supported by the U. S. Army Research Office.

[1] L. L. Chang, L. Esaki, and R. Tsu, Appl. Phys. Lett. 24, 593 (1974).
[2] T. C. L. G. Sollner, W. D. Goodhue, P. E. Tannenwald, C. D. Parker, and D. D. Peck, Appl. Phys. Lett. 43, 588 (1983).
[3] P. D. Coleman, J. Freeman, H. Morkoç, K. Hess, B. Streetman, and M. Keever, Appl. Phys. Lett. 40, 493 (1982).
[4] R. F. Trambarulo, International Solid-State Circuits Conference, Philadelphia, PA, 1961.
[5] C. A. Burrus, Proc. IEEE 54, 575 (1966).
[6] M. E. Hines, Bell Syst. Tech. J. 39, 477 (1960).

APPENDIX III

Heterodyne Experiments from Millimeter Wave to Optical Frequencies Using GaAs MESFETs Above f_T*

A. Chu, H. R. Fetterman, D. D. Peck, and P. E. Tannenwald

Lincoln Laboratory, Massachusetts Institute of Technology
Lexington, Massachusetts 02173

Abstract

Response of GaAs FETs in mm-wave and optical heterodyne experiments has been obtained at frequencies above the frequency of unity current gain, f_T. In the mixing of two visible lasers, beat frequencies as high as 300 GHz have been observed. These high IFs were down converted to microwave frequencies by radiatively coupling mm-wave local oscillators into the gate region.

Introduction

Substantial efforts are currently being devoted to extending GaAs MESFET operation into the millimeter frequency regime. To date, experimental 0.25 μm gate length devices have exhibited useful gain up to 40 GHz.[1] In the present work GaAs FETs are investigated by operating them as mixers and detectors at much higher frequencies, significantly above f_T. Although a number of studies involving visible radiation have been made using picosecond pulses,[2] the emphasis here is the response to CW sources.

Our results indicate that GaAs FETs can be used as sensitive and versatile detectors and mixers of millimeter wave and optical radiation. As millimeter mixers results have been obtained up to 350 GHz. Exploiting this millimeter wave responsivity, optical mixing between two lasers has been demonstrated with IF frequencies up to 300 GHz.

Device Description and Experimental Procedures

Devices used in the experiments are 0.5 μm gate length MESFETs with a total gate width of 104 μm. The gate fingers are located in a drain-source spacing of ~4 μm. Gate capacitance and transconductance are typically 0.06 pF and 9.5 mS, respectively. Consequently, f_T is approximately 25 GHz. A photomicrograph of a typical device is shown in Fig. 1a. The FETs are mounted in the common source configuration and biased in the linear region. The optical and millimeter wave signals are coupled radiatively into the gate region of the FET, and the IF frequency is detected at the drain terminal in a 50Ω system. The gate terminal is only used if the IF is down converted further by a second local oscillator in the microwave range. Otherwise, the gate terminal is connected to ground via a 50Ω resistor. The 3-way mixing of two optical signals with either a microwave signal or a millimeter wave signal is illustrated in Fig. 2.

Millimeter Wave Mixing

In the millimeter wave and submillimeter wave frequency range the signal is radiatively coupled into the gate region by the fields of a closely spaced waveguide. The coupling is maximized when the E-field is orthogonal to the gate stripe, as indicated in Fig. 1a. Video detection has been obtained up to 800 GHz by this method. Harmonic mixing was performed by combining spatially the fields of a 350 GHz carcinotron with that of a 70 GHz klystron in the vicinity of the gate region. The detected IF is the difference frequency between the ~350 GHz signal and the 5th harmonic of the 70 GHz local oscillator and was typically in the range of 2 to 4 GHz. In the harmonic mixing experiment the signal to noise ratio for the detected IF response was typically on the order of 45 dB.

Optical Mixing

Since millimeter wave detection and mixing has been demonstrated, it becomes feasible to examine optical mixing at very high IF frequencies. Mixing in the optical region was performed by focusing a He-Ne laser at 6328 Å and a tunable stabilized dye laser pumped by an Ar^+ ion laser onto the vicinity of the gate with a ~3 μm diffraction limited spot. Power levels for the He-Ne laser and dye laser were 1 mW and 50 mW, respectively. As an optical detector the signal level was on the order of 60 mV. A summary of mixing experiments in the optical region showing the relevant spectral ranges involved is illustrated in Fig. 3. The stabilized dye laser was tuned away from the He-Ne laser to produce IF frequencies ranging from 100 MHz to 300 GHz. In order to cover this wide IF range three conversion techniques were used in different frequency regimes. Below 20 GHz the IF response was detected directly using a spectrum analyzer. Between 20 and 40 GHz the IF response was heterodyned down to 500 MHz by feeding a microwave local oscillator into the gate terminal of the FET. The power of the microwave local oscillator used

*This work was sponsored by the U.S. Army Research Office and the U.S. Air Force (with specific support by AFOSR).

CH1784-8/82/0000-0025$00.75 © 1982 IEEE

was approximately 200 mW. Between 40 and 300 GHz, down conversion of the millimeter wave IF signal was achieved by coupling the millimeter wave LO from a carcinotron into the gate region by means of a closely spaced waveguide, as shown in Fig. 4.

As a special case of optical mixing using only one laser, two modes of a He-Ne laser were also mixed in an FET to produce an IF signal of 641 MHz. Plots of the detected IF signal were obtained by scanning the laser beam over the device in order to define the active region as shown in Fig. 1b. Reduced response has also been observed from the mode mixing of a Nd:YAG laser at 1.06 μm, ie., below the GaAs bandgap energy.

Discussion of Results

The frequency limit in most GaAs FET applications arises from the fact that the signal is fed into the gate terminal, which is loaded by the depletion layer capacitance, C_g. As a result, the time constant associated with C_g and the transconductance, g_m, dominates the frequency response of the device. The frequency of unity current gain is given by $f_T = g_m/2\pi C_g$ and consequently is the primary frequency limit when the signal is fed directly into the gate terminal. However, f_T is not necessarily the upper limit when signals are radiatively coupled into the device.

Coupling optical signals into an FET has been reported previously. Optically induced variations of drain current[3,4,5], gate capacitance[6], pinch-off voltage[3], S-parameters[7], and back-gating[5] have also been studied. Applications of the photo-induced effect for tuning the frequency of GaAs FET oscillators[6,8] and for use as high-speed optical detectors[4,7,9,10] have also been demonstrated. The photoresponse mechanism of GaAs FETs proposed by Sugeta and Matsushima[11] is shown in Fig. 5. Optical illumination generates carriers in the depletion layer, which are then swept out by the electric field, producing a photocurrent i_{ph}. The associated gate photovoltage in turn modulates the depletion layer, varying the drain current via the transconductance of the FET. Since modulation of the drain current is based on the photogenerated voltage at the gate terminal, the frequency response of a FET to an intensity modulated optical excitation will still be constrained by f_T — essentially the same limit as for an FET in a microwave application where the input signal is connected directly to the gate terminal. The above mechanism can be extended to explain optical mixing at IF frequencies below f_T, such as mixing of two modes of a He-Ne laser in an FET to produce carriers at the beat frequency of 641 MHz.

For IF signals significantly above f_T it is not possible for the depletion layer to follow the beat frequency because of long time constants associated with the large depletion layer capacitance. Hence a different mechanism must be responsible for the observed mixing, such as photoconductivity with consequent modulation of the depletion layer and photo-induced effects at the depletion layer edges of the gate. If mixing is produced by a net change in photo-induced carrier density in the FET channel, then the rapid removal of one carrier type from the active device area is required. Both the lifetime and transit time of electrons through the gate region are too long to account for the observed high frequency response. Two possible mechanisms for more rapid carrier removal are the trapping of holes by defect centers or the differences of sweep-out rate of electrons and holes by the electric field. Trapping of holes has been proposed previously to explain the increase of gate capacitance under optical illumination.[6] Then modulation of the drain current results from variation of the channel thickness at the depletion layer edge. In Fig. 6 the response of the depletion layer under the gate to an applied E-field is shown. Because of the built-in potential of the Schottky barrier, charges do not come from the gate metal, but rather they originate near the boundary of the depletion layer. If the charges induced by the radiatively coupled E-field are confined to the edges of the gate, then modulation of the current in the channel takes place. The high frequency response follows by virtue of the small incremental capacitance associated with the depletion layer edge rather than with the large capacitance of the entire depletion layer. In the case of millimeter wave mixing a second E-field is radiatively coupled in, to down-convert to IF frequenies which are detected at the drain terminal. Mixing could arise from nonlinearities in the junction or from channel modulation effects.

Summary and Conclusions

A number of experiments are in progress to determine the relative importance of the mechanisms giving rise to mixing in an FET over a broad frequency range. More complex mechanisms than those discussed above may have to be invoked to explain the response that has been observed in the saturated current regime, and the reduced response observed from the mode mixing of a Nd:YAG laser at 1.06 μm, below the band gap energy.

In view of the inefficient coupling of millimeter wave and optical signals into the device, it seems appropriate to consider device configurations that might provide tighter coupling. Gamel and Ballantine[3] have proposed coupling the optical signal into the FET using an optical waveguide positioned parallel to the FET gate. The analogous device for mixing in the millimeter wave region would utilize a dielectric waveguide parallel to the gate. Devices without gates could also be fabricated to test the relative importance of the depletion layer in optical and millimeter wave mixing. A second possibility is using GaAs optical or millimeter waveguide on a layer of SiO_2 and thereby fabricating the device as an integral part of the guide. GaAs and InP optical waveguides fabricated using epitaxial overgrowth have been reported by Leonberger and coworkers.[12] We suggest the fabrication of FETs on an n-type layer grown over the semi-insulating waveguiding structure. In

this second approach the waves would be propagating within the device rather than coupling to the fringing fields. Experimental devices such as those described may provide better coupling to the optical or millimeter waves, as well as a means to obtain additional data for the understanding of the physical mechanisms which produce mixing in FETs at high frequencies.

Acknowledgment

A. Gopinath contributed to the design and fabrication techniques of the 0.5 μm gate FETs. M. W. Pierce, G. A. Lincoln and G. R. Durant provided valuable technical assistance in the fabrication of the FETs. W. Macropoulos and A. R. Forte contributed their expertise in packaging the devices. The authors are indebted to W. E. Courtney, A. J. Seeds and R. A. Murphy for many technical discussions.

References

1. E. T. Watkins, H. Yamasaki, and J. M. Shellenberg, ISSCC Digest of Technical Papers, pp. 198-199, Feb. 1982.
2. P. R. Smith, D. H. Auston, and W. M. Augustyniak, Appl. Physics Lett., vol. 39, pp. 739-741, Nov. 1981.
3. J. Graffeuil, P. Rossel, and H. Mortinot, Electronic Lett., vol. 13, pp. 439-440, July 1979.
4. J. C. Gammel and J. M. Ballantyne, IEDM Digest of Technical papers, pp. 120-123, Dec. 1978.
5. W. D. Edwards, Elect. Dev. Lett., vol. EDL-1, pp. 149-150, Aug. 1980.
6. J. J. Sun, R. J. Gutman, and J. M. Borrego, Solid-State Electronics, vol. 24, pp. 935-940, Oct. 1981.
7. J. J. Pan, SPIE, vol. 150, Laser and Fiber Optics Communications, pp. 175-184, 1978.
8. A. A. Salles and J. R. Forrest, Appl. Physics Lett., vol. 38, pp. 392-394, March 1981.
9. J. M. Osterwalder, and B. J. Rickett, Proc. IEEE, vol. 69, pp. 966-968, June 1979.
10. C. Baak, G. Elze, and G. Walf, Electron. Lett.,vol. 13, p. 193, March 1977.
11. T. Sugeta and Y. Matsushima, Japanese J. of Appl. Phys., vol. 19, pp. L27-L29, Jan. 1980.
12. F. J. Leonberger, C. O. Bozler, R. W. McClelland, and I. Melngailis, J. Appl. Phys. Lett., vol. 38, pp. 313-315, Mar. 1981.

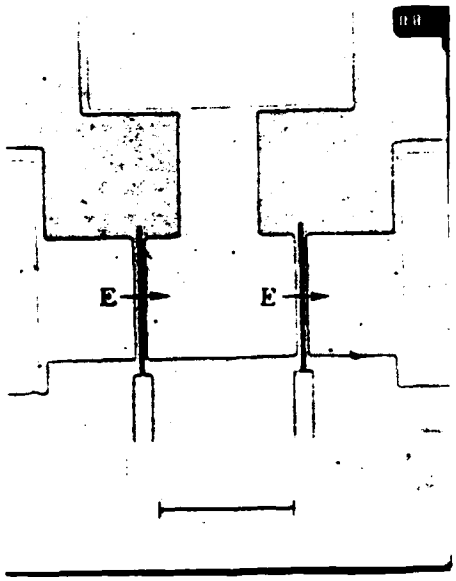

(a)

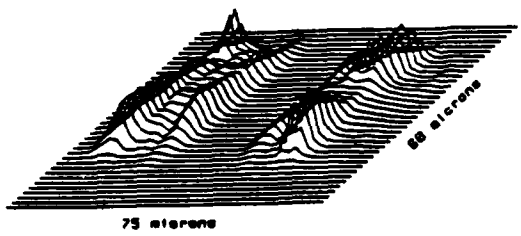

(b)

Figure 1. (a) Photomicrograph of 0.5 μm x 104 μm gate GaAs FET. b) Scanning plots of beat frequency from mixing two modes of a He-Ne laser in 0.5 μm gate device.

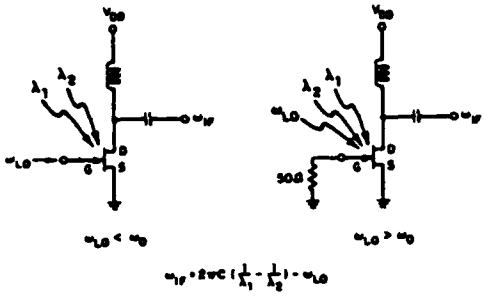

Figure 2. Examples of 3-way mixing: (a) Two optical signals and a microwave LO. (b) Two optical signals and a millimeter wave LO.

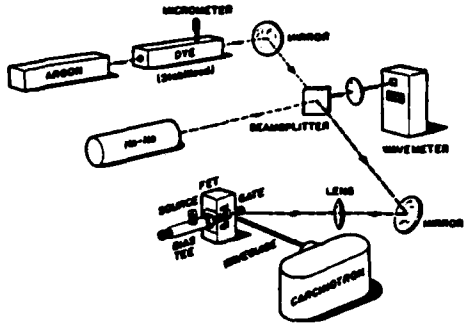

Figure 4. Mixing experiment using two lasers and a millimeter wave LO.

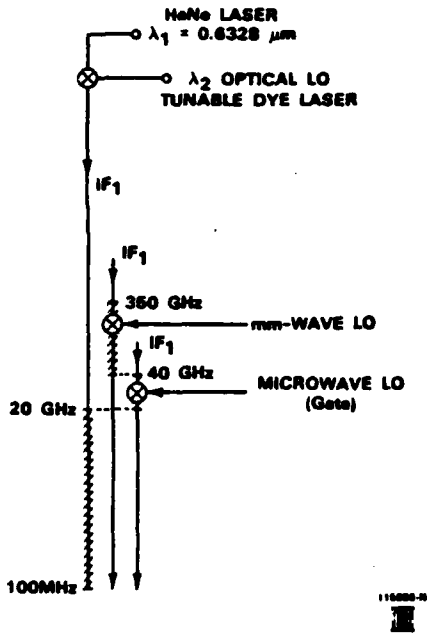

Figure 3. Summary of mixing experiments in the optical region showing the relevent spectral regions involved.

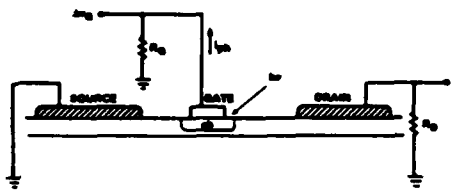

Figure 5. Photoresponse mechanism after Sugeta and Matsushima.

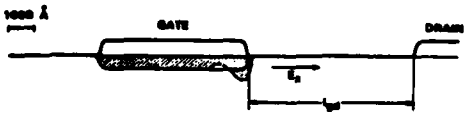

Figure 6. Response to an applied millimeter wave E-field in the depletion layer.

Heterodyne Radiometry Measurements of the 557 GHz H_2O Rotational Line

GERALD F. DIONNE, HAROLD R. FETTERMAN, NEAL R. ERICKSON, CHRISTOPHER D. PARKER, AND JAMES F. FITZGERALD

Abstract—A high-resolution heterodyne radiometer that utilizes a crossed-guide harmonic mixer pumped by a 300 GHz carcinotron as a local oscillator has been developed for submillimeter wavelengths. Previous investigations of the radiation transfer properties of spectral lines in supersonic gas flow have been extended to longer wavelengths using the tunability of this system. With less than 2 mW of fundamental local oscillator power, traces of the 557 GHz ortho-H_2O rotational transition ($1_{10} \leftarrow 1_{01}$), Doppler-broadened to only a few MHz, were observed in absorption against a continuum background.

IN earlier studies of the radiation transfer characteristics of isentropically expanding H_2O molecules, a Schottky-barrier GaAs diode mounted in a corner reflector configuration [1] was used as the first-stage mixer of a high-resolution submillimeter-wave heterodyne radiometer. This instrument, with a resolution capability better than 1 MHz, was used to make the first rotational excitation temperature measurements of the para-H_2O 752 GHz ($2_{11} \leftarrow 2_{02}$) line (see Fig. 1) in supersonic flow [2], [3]. A CO_2-pumped HCOOH laser at 761 GHz proved to be a convenient source of local oscillator (LO) power, providing a manageable 9 GHz intermediate frequency. Although this system was highly sensitive at the wavelength required for the 752 GHz line, obtaining sufficient local oscillator power at the wavelengths of other lines, such as the intense $1_{10} \leftarrow 1_{01}$ transition of ortho-H_2O at 557 GHz (see Fig. 1), proved to be extremely difficult. It was for this reason that a highly tunable harmonic system was developed.

Backward-wave oscillators (BWO or carcinotron) are readily available with acceptable power levels for this application up to 400 GHz. Furthermore, the concept of using second-harmonic mixing for radiometric measurements has been demonstrated at 600 GHz [4]. In the present work, a highly sensitive crossed-guide doubler [5], based on a design scaled from lower frequencies [6], was used to establish the feasibility of this type of high-resolution spectral-line radiometric measurement required for investigations of molecular temperatures in supersonic gas flows. This doubler, shown in Fig. 2, employs fundamental waveguide at 1 and 0.5 mm, separated by a coaxial choke to isolate the harmonics. In combination with a 300 GHz carcinotron, this doubler/mixer was used to replace the corner reflector Schottky diode and the HCOOH laser of the original experiment.

As outlined in the apparatus sketch of Fig. 3, continuum radiation from a Hg-arc lamp was transmitted through the supersonic flow of an expanding water vapor jet in a high vacuum chamber. Outside of the TPX exit window, the signal entered a N_2 dry box (required to remove atmospheric water that would mask the spectral absorption effects inside the chamber), and was focused into the 0.5 mm waveguide of the mixer. With a fundamental frequency of 281.5 GHz, the harmonic mixing occurred between 563 GHz and the 557 GHz signal to produce a 6 GHz intermediate frequency (IF) for the first stage of the double heterodyne receiver.

After preamplification and filtering, a second mixer was used to beat the IF down to ~3 GHz with a tunable *X*-band frequency generator. The receiver resolution was fixed by a 3 GHz waveguide cavity filter with a 1 MHz passband. Signal processing and recording were then carried out by phase sensitive detection similar to that of the original experiments [2], [3].

With a combination of carcinotron and harmonic mixer, a double-sideband system noise temperature of 50 000 K was measured at the fundamental frequency of 281.5 GHz required in the experiment. Since a large part of the 50 000 K was generated by the carcinotron itself, substantial improvements in sensitivity would be realized by greater filtering of the local oscillator. This temperature was approximately double the value of 23 000 K previously measured in testing at 285 GHz [5]. Since the carcinotron maximum available power at 281.5 GHz was about a factor of ten lower than the 2 mW at 285 GHz, it is logical to conclude that the receiver was LO starved in these experiments and that increases in the fundamental power level could result in further sensitivity improvements.

In spite of the limited LO power and sensitivity, the signal-to-noise ratio was sufficient to trace line shapes with a 1 s integration time on the phase sensitive detector. As presented in Fig. 4, the preliminary trace of the H_2O absorption line at 557 GHz had a linewidth of about 6 MHz, and reached a rotational excitation temperature (assuming 100 percent optical depth) of about 60 K. The theoretical Doppler broadening of the situation of diverging streamlines in an isentropic expansion would be estimated at about 4 MHz at 557 GHz [2], [3]. The high value of experimental linewidth arises from a 60 Hz ripple in the carcinotron power supply voltage that caused a variation (~3 MHz) in the output frequency.

As explained in earlier works [2], [3], the rotational excitation temperature is expected to remain in equilibrium with the

Manuscript received September 1, 1983. This work was supported in part by the Department of the Army, United States Army Research Office.

G. F. Dionne, C. D. Parker, and J. F. Fitzgerald are with the Lincoln Laboratory, Massachusetts Institute of Technology, Lexington, MA 02173.

H. R. Fetterman is with the Department of Electrical Engineering, University of California, Los Angeles, CA 90024.

N. R. Erickson is with the Five College Radio Astronomy Observatory, University of Massachusetts, Amherst, MA 01003.

0018-9197/84/0300-0188$01.00 © 1984 IEEE

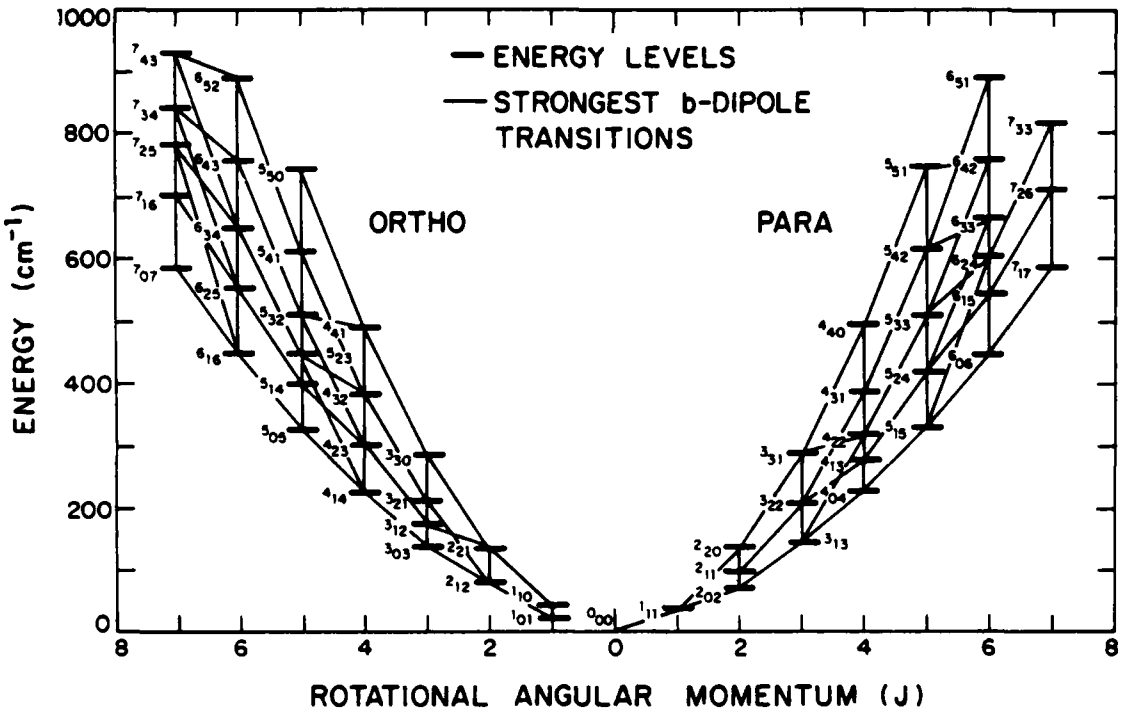

Fig. 1. Water molecule rotational energy levels.

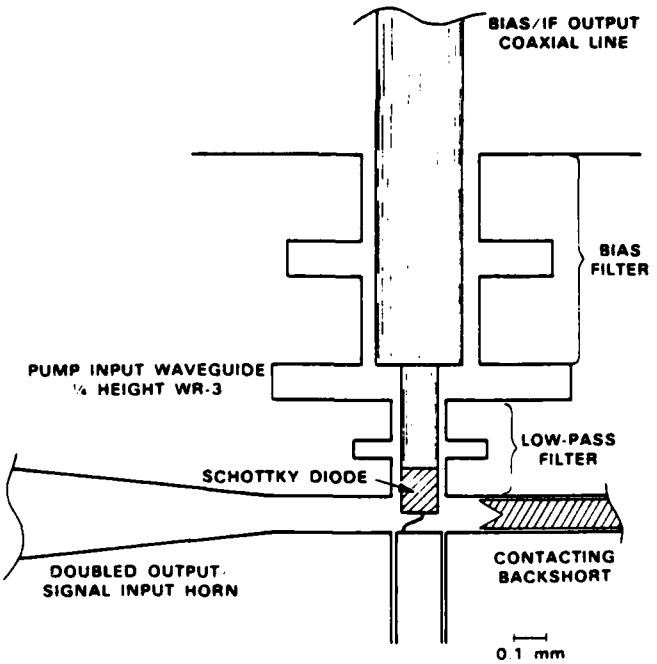

Fig. 2. Cross section drawing of the submillimeter-wave doubler/mixer.

molecular translational temperature of the isentropic expansion, and to cool to below room temperature within a few nozzle diameters downstream. In this case, the nozzle size was 2 cm in diameter and the observations were made along a radiometer line-of-sight 50 nozzle diameters from the jet exit plane. Changes in the 557 GHz rotational temperature with distance downstream and details of the line profile are subjects of continuing investigations employing this new radiometric capability.

In future experiments, substantial improvements in resolution and sensitivity through the use of a filter bank are expected to make possible more precise measurements of the line profile. In addition, with the present success achieved from less than 2 mW of fundamental LO power, it now seems likely that the output of a solid-state power source at 94 GHz may be tripled by solid-state circuitry to supply sufficient power for replacing the carcinotron in a next generation of this radiometer.

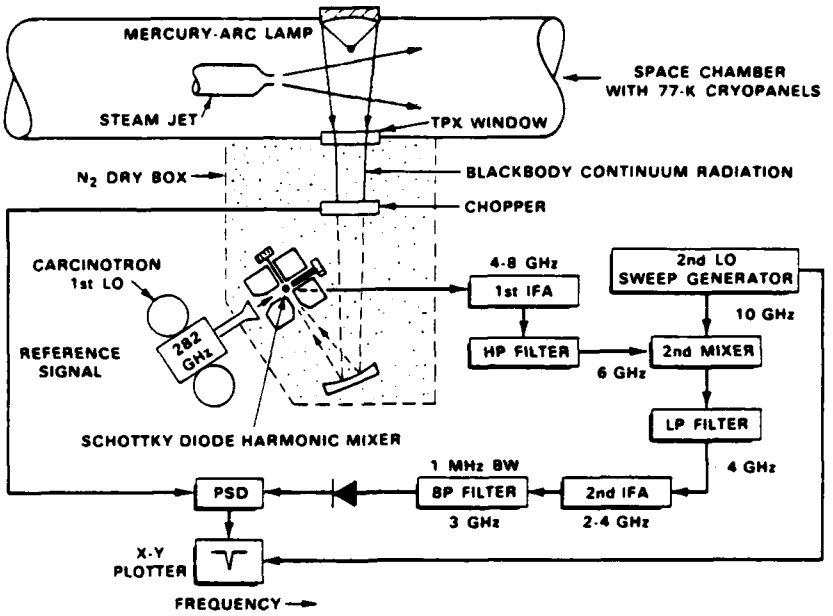

Fig. 3. Diagram of vacuum chamber, steam jet, and the 1 MHz resolution heterodyne radiometer for measuring characteristics of the 557 GHz H_2O rotational in a supersonic flow.

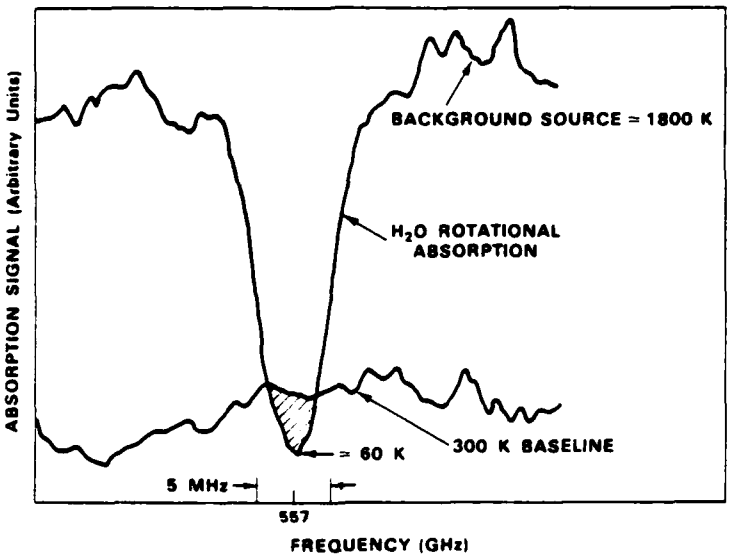

Fig. 4. Experimental trace of the 557 GHz ortho-H_2O rotational line in supersonic flow. Since the TPX exit window had a transmissivity of 0.67, this voltage trace could not be converted to temperature without applying the appropriate corrections for the window emissivity. For this reason, only the background temperature (~1800 K) and the temperature at line center (~60 K) relative to the 300 K reference chopper have been indicated in this figure.

Acknowledgment

The authors are grateful for the assistance and support of Dr. P. E. Tannenwald, R. W. Sudbury, Dr. J. L. Ryan, C. L. Gillaspie, and D. D. Peck. Guidance on theoretical aspects of this research was contributed by Dr. M. M. Litvak of the Jet Propulsion Laboratory, California Institute of Technology, Pasadena.

References

[1] H. R. Fetterman, P. E. Tannenwald, B. J. Clifton, C. D. Parker, W. D. Fitzgerald, and N. R. Erickson, "Far-IR heterodyne radiometric measurements with quasioptical Schottky diode mixers," *Appl. Phys. Lett.*, vol. 33, pp. 151-154, 1978.

[2] G. F. Dionne, J. F. Fitzgerald, T.-S. Chang, M. M. Litvak, and H. R. Fetterman, "Radiometric observations of the 752.033-GHz rotational absorption line of H_2O from a laboratory jet," *Int. J. IR MM Waves*, vol. 1, pp. 581-595, 1980.

[3] —, "Heterodyne detection of the 752.033-GHz H_2O rotational absorption line," in *Proc. Int. Conf. Heterodyne Syst. Technol.*, Williamsburg, VA, 1980, NASA Conf. Pub. 2138, pp. 249-262.

[4] S. Y. Chang and J. D. Lester, "Radiometric measurement of atmospheric absorption at 600 Gc/s," *Proc. IEEE*, vol. 54, pp. 459-461, 1966.

[5] N. R. Erickson and H. R. Fetterman, "Single mode waveguide submillimeter frequency multiplication and mixing," in *Proc. 4th High Temperature Plasma Diagnostics Topical Conf.*, Boston, MA, Aug. 1982, *Bull. Amer. Phys. Soc.*, vol. 27, p. 836.

[6] N. R. Erickson, "A 200-300 GHz heterodyne receiver," *Dig. IEEE 1980 Int. Microwave Symp.*, Washington, DC, 1980, pp. 19-20.

APPENDIX V

THE ASTROPHYSICAL JOURNAL, 260:584–589, 1982 September 15
© 1982. The American Astronomical Society. All rights reserved. Printed in U.S.A.

CO ($J = 6 \rightarrow 5$) DISTRIBUTION IN ORION AND DETECTION IN OTHER GALACTIC SOURCES

G. A. KOEPF[1]
Phoenix Corporation
D. BUHL[1] AND G. CHIN[1]
NASA/Goddard Space Flight Center
AND
D. D. PECK,[1] H. R. FETTERMAN, B. J. CLIFTON, AND P. E. TANNENWALD
Lincoln Laboratory, Massachusetts Institute of Technology
Received 1981 November 18; accepted 1982 March 5

ABSTRACT

The profile of the CO line in Orion has been studied at 691 GHz with the NASA infrared telescope at Mauna Kea using a laser heterodyne receiver. The line from the BN/KL region is very broad and has a peak temperature of $T_A^* = 180$ K. Away from BN/KL, the emission line becomes narrow, and the intensity falls off rapidly. Several other galactic sources were also detected.

Subject headings: interstellar: molecules — nebulae: Orion Nebula

I. INTRODUCTION

In 1980 May the first detection of the 691 GHz ($J = 6 \rightarrow 5$) transition of CO was made in Orion using the NASA Infrared Telescope Facility (Fetterman *et al.* 1981). The relatively broad (FWHM = 26 km s^{-1}), hot (100 K) emission that was observed was identified with the so-called "plateau source" that is seen in the spectra of several other molecules (HCN, SO_2, SiO, etc.). In contrast with observations of CO at lower frequencies (Phillips *et al.* 1977 and 1979), there was an apparent total absence of the prominent narrow-line feature. A related question was the correlation of this high rotational state of excited CO with the gas kinetic temperature and hydrogen density and whether it is localized to the region near the cloud core. Finally, this observation pointed to the possibility that regions of comparable molecular excitation ($T > 100$ K) may be found in the cores of other molecular clouds.

In the current observations made in 1981 February at the Infrared Telescope Facility (IRTF) on Mauna Kea, each of these points has been addressed. The spatial CO distribution has been investigated with high resolution (35″). Areas with both narrow line features and broad "plateau" emission have been identified. Other sources, with an antenna temperature almost an order of magnitude cooler, have been measured and compared with lower frequency studies. An attempt has been made to analyze the data quantitatively with a rate equation approach and to fit it to a kinetic model.

[1]Visiting Astronomer at the Infrared Telescope Facility which is operated by the University of Hawaii under contract from the National Aeronautics and Space Administration.

II. INSTRUMENTATION AND CALIBRATION

The system used here, described in detail elsewhere (Fetterman *et al.* 1981; Goldsmith *et al.* 1981), employs a heterodyne receiver developed for the submillimeter. It consists of a corner cube Schottky diode (Fetterman *et al.* 1978) serving as the mixer, with a stabilized optically pumped molecular laser (Koepf, Fetterman, and McAvoy 1980) serving as the local oscillator. The 1.4 GHz IF amplifier is a field effect transistor with a noise temperature of approximately 50 K. The entire system, including an IF matching network (and bias Tee), had a noise temperature of 3900 K double sideband at 432 μm.

The number of the 5 MHz wide channels in the IF filter bank was increased over the earlier experiment to 64 in order to improve the baseline accuracy. Instead of position switching, which was used in the first experiment, the chopping secondary with a 120″ excursion was used to improve the signal-to-noise ratio and to reduce baseline drift. The extended distribution of excited CO introduced a degree of reference beam contamination with this approach. We will study this problem during a future observing period to determine how severe it is.

During the experiment particular attention was given to calibration of absolute temperatures and to determination of the beam size and shape. Daily measurements were made of the total amount of precipitable water vapor using a Westphal near-infrared solar absorption meter. In addition, atmospheric transmission measurements were made at 691 GHz by recording the atmospheric emission at various elevation angles. This provided the absorption coefficients (τ) at 1 air mass

(Fetterman *et al.* 1981). These measurements were then compared with direct observations of the Moon and Jupiter every few hours. From these comparisons we derived an absorption coefficient for each observing day which varied from $\tau = 0.6$ to 1.2. These values indicate water vapor amounts of < 1 precipitable mm in a vertical column. The absorption at 691 GHz during our observing period was exceptionally low, even for a site like Mauna Kea. All of the observations were then corrected using the derived coefficient, the elevation angle, and the measured telescope efficiency.

The absolute intensity scale was derived from repeated observations of Jupiter assuming a continuum temperature of 130 K for the planet (Wright 1976). At the time of observation Jupiter was 40″ in diameter. A map of Jupiter showed that the beam was circularly symmetric with a relatively low beam efficiency (20%) caused by spillover of the telescope secondary and led to a determination of 35″ for the beam diameter (FWHM).

III. OBSERVATIONS

a) Orion BN/KL

Figure 1 illustrates the CO spectra at two points in Orion at the BN/KL position and 1′ south. These spectra were taken by beam switching the telescope for 6 minutes. Figure 2 shows part of the data obtained from our observations of Orion as a function of position. The measurements, which were repeated on different days, indicated that the intensity scale was consistent to ±20%. The mapping of CO ($J = 6 \rightarrow 5$) in Orion A shows the localized plateau emission at position ($\alpha_{1950} = 5^h32^m47^s$, $\delta_{1950} = 5°24'21''$) in addition to the extended narrow emission observed in CO mappings at lower frequencies. In comparison with earlier CO measurements at $J = 1$, 2, and 3, there are three apparent differences (see Fig. 2): (1) the narrow emission is not homogeneously structured; (2) the plateau emission is more pronounced, and (3) the plateau exhibits a different profile and a dip in the center rather than a spike. Our antenna temperature of 70–80 K for the extended emission agrees qualitatively over most of the region with lower frequency data. There is an apparent falloff in intensity away from BN/KL. A slight E-W asymmetry in the distribution is also observed (Fig. 2). It is most pronounced at the 0″ and −30″ decl. positions. In addition to regions of plateau and narrow line emission, there are locations where both are simultaneously observed such as Fig. 2*a* and Fig. 2*b* −30″, $\Delta RA = 0$. Signals appearing at Fig. 2*b* −120″ and −150″ decl. are interpreted as indicating the differential between two velocity components of excited CO. At several positions south of BN we measured temperatures as high as 120 K. The $3 \rightarrow 2$ and $4 \rightarrow 3$ transition of CO has also shown enhanced emission at BN (Phillips *et al.* 1977; Huggins *et al.* 1981; van Vliet 1981). However, these hotter regions in the extended spike emission have not been observed at lower frequencies.

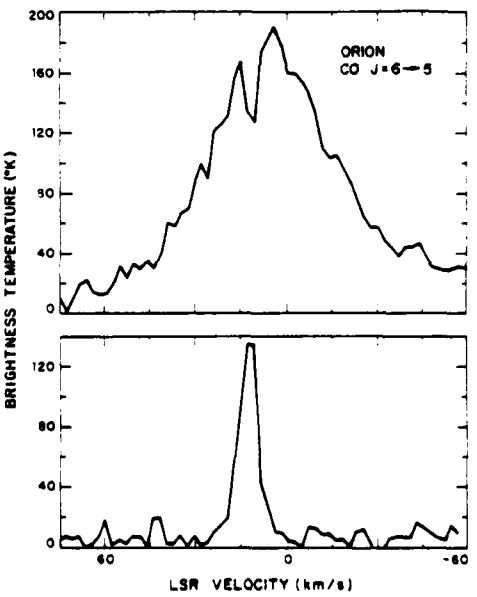

FIG. 1.—CO line profile in the center of the BN region of Orion. The central dip in the line is either due to self-absorption or a weak emission line in the reference beam. The CO emission spike 1′ south is also shown. Note the large T_A^* obtained for this position.

In the center position (BN) we found an antenna temperature of 180±36 K for the plateau emission, which is somewhat higher than our previous result (Fetterman *et al.* 1981; Goldsmith *et al.* 1981). The velocity distribution of the earlier measurement of the $J = 6 \rightarrow 5$ transition differs somewhat from our present profile: the FWHM was only 26±5 km s^{-1} as compared to 38±5 km s^{-1}, and no dip appeared close to line center. The smaller width could be partly attributed to the uncertainty in the earlier baseline. Also, the position of observation for our first spectra may have been as far as 30″ E of the BN peak, which was the center of our current observations.

Absence of a central spike feature might indicate absorption along the line of sight. However, as we noted in the calibration section, the most consistent explanation for the origin of the observed dip in the broad emission feature is subtraction of narrow CO emission in the reference beam. To clarify this concept the observations taken along the central north-south ridge are also shown in the figure for a reference 2′ in the west direction. The differences in the two directions of the central dip and the relative size of the narrow line emission could be interpreted by a subtraction of CO emission in the reference beam. This implies that the contamination is equal to the absorption $T_A^* \sim 40$ K. The lateral extension of the plateau emission, when

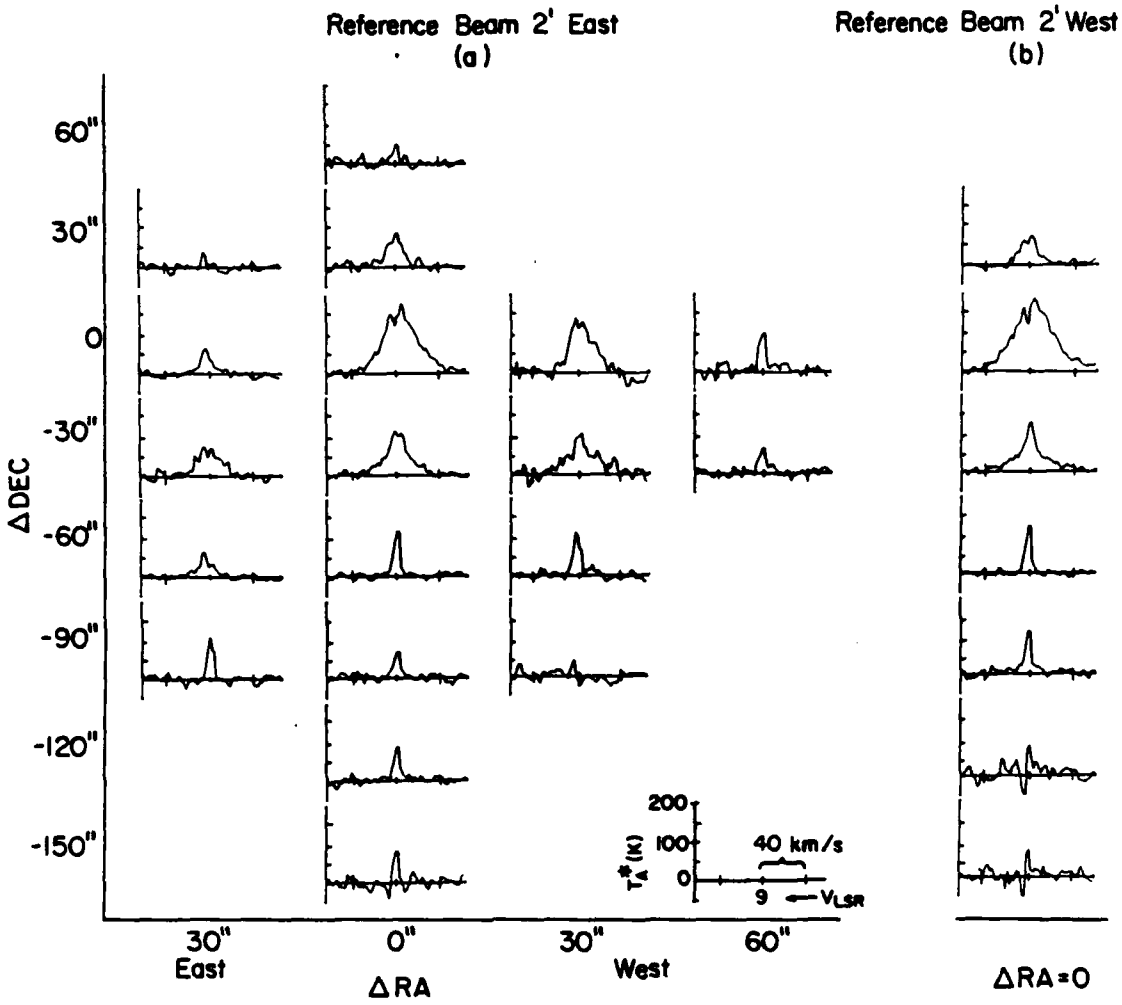

FIG. 2.—CO emission $J = 6 \rightarrow 5$ from Orion as a function of displacement from BN. Along the north-south ridge the results of referencing the chopping secondary in the west direction are also shown. The observations indicate a slight asymmetry in the narrow line emission distribution which is clearly seen in Fig. 2*b* 0″ and −30″ decl.

assumed to have a Gaussian velocity profile, is about 45″ in right ascension and 35″ in declination. This is in close agreement with earlier mappings at lower J levels (Phillips *et al.* 1977; Solomon, Huguenin, and Scoville 1981). The plateau emission, when separated from the narrow feature and fitted to a Gaussian, is hotter at $J = 6 \rightarrow 5$ than at lower J levels, both at the center and in the wings. At 25 km s^{-1}, almost a perfect J^2 law is obtained for the antenna temperatures, consistent with an optically thin line at LTE. At line center the ratio $(1 \rightarrow 0):(2 \rightarrow 1):(3 \rightarrow 2):(6 \rightarrow 5)$ is about 1:2:4:20 and can be viewed as the deviation from LTE for regions of different excitations or evidence of some optical thickness at $J = 6 \rightarrow 5$. The data are listed in Table 1.

b) Other Sources

Several other sources were observed in these runs and are shown in Figure 3 and compared with other J levels in Table 1. They do not exhibit the large intensity increase observed in the $J = 6 \rightarrow 5$ CO line in Orion. This indicates that either the lines are optically thick in these sources or the region has a lower density and is sub-LTE in the $J = 6$ levels. The profiles in IRC + 10216 appear very similar to the $J = 1 \rightarrow 0$ and $2 \rightarrow 1$ transitions of CO (Kuiper *et al.* 1976; Wannier *et al.* 1979). Sgr B2 shows peaks in the emission at 50 and 80 km s^{-1}, which resemble those observed in HCN and HCO^+ in Sgr B2 (Hollis *et al.* 1975; Linke *et al.* 1977). DR 21 OH shows

TABLE 1

CO ($J = 6 \rightarrow 5$) INTENSITIES CORRECTED FOR TELESCOPE EFFICIENCY AND ATMOSPHERIC ABSORPTION (T_A^*)

Source	α (1950)	δ (1950)	V_{LSR} (km s^{-1})	CO (1 → 0) (K)	CO (2 → 1) (K)	CO (3 → 2) (K)	CO (6 → 5) (K)
Orion[a]	5^{h}32^{m}47.0	−5°24′21″	9	9[a,b]	20[a,c]	35[a,d]	180[a]
Orion (spike)	5 32 47.0	−5 25 21	9	85	93	79[e]	120
OMC 2[b]	5 33 00	−5 12 34	9	45[e,f]	47[f]	...	10
NGC 2023	5 39 10.0	−2 17 49	10	...	...	...	20
NGC 2024	5 39 12.0	−1 55 42	9	40[f]	31[f]	...	25
IRC 10216[d]	9 45 14.8	13 30 41	−22	6[g]	18[h]	2[e]	15
Sgr B2[f]	17 44 11	−28 22 30	50,80	15[i]	13[i]	...	25
W49	19 07 53	9 01 00	7	...	...	...	20
DR 21[c]	20 37 14	42 12 00	−5	25[f]	20[f]	17[e]	40

[a] Temperature of broad plateau feature in Orion.
[b] Zuckerman, Kuiper, and Rodriguez Kuiper 1976.
[c] Wannier and Phillips 1977.
[d] Phillips *et al.* 1977.
[e] Erickson 1979.
[f] Plambeck and Williams 1979.
[g] Kuiper *et al.* 1976.
[h] Wannier *et al.* 1979.
[i] Phillips *et al.* 1979.

an apparent double line similar to the profile of the $J = 3$–2 CO line (Phillips *et al.* 1981) and the HCO^+ line (Hollis *et al.* 1975); however, the data of Phillips *et al.* refer to a position 3′ south of our data. Although our high spatial resolution (35″) permits us to observe various hot H II regions, the different angular sizes of these sources introduce various degrees of beam dilution. Further studies of these clouds will reveal the effect of source structure on the measured intensity. An effort is being made to understand these systems using a rate equation model analogous to that which will be described in the next section. Some of the sources observed here have also been examined at higher J levels (Storey *et al.* 1981). The upper limits for excitation temperatures obtained there are consistent with the measurements reported here.

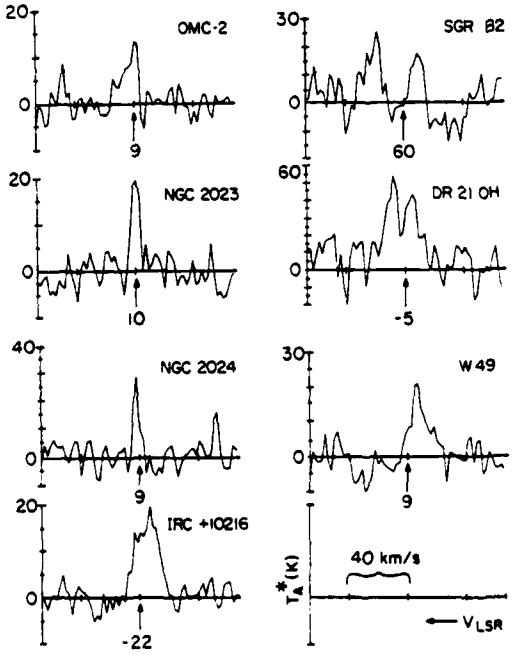

FIG. 3.—Several sources of $J = 6 \rightarrow 5$ CO emission at 691 GHz. Although the signals are weak, the general shapes are consistent with observations at lower frequencies. The integration time for these runs was 6 minutes per scan.

IV. DISCUSSION

The kinetic processes that cause the hot plateau emission in Orion have been the subject of extensive speculation and modeling. The most widely applied models are based on large scale velocity gradient structures (Goldreich and Kwan 1974; Scoville and Solomon 1974). The $J = 3 \rightarrow 2$ and $2 \rightarrow 1$ plateau profiles have been matched with a differential expansion model by Kwan and Scoville (1976) and by Wannier and Phillips (1977), respectively. Our $J = 6$–5 profile can be fitted to this model only by assuming a substantially higher velocity gradient. The detection of molecular hydrogen emission has recently led to the model of a shock wave expanding into the molecular medium (Kwan 1977). For conversion of the H_2 molecules in the hot shock front, a maximum shock velocity of 24 km s^{-1} has to be imposed. The detection of CO emission from high J levels (Watson *et al.* 1980) has also been attributed to such postshock regions where the kinetic temperature has decreased to about 1000 K (Storey *et al.* 1981). Unfortunately, these observations lack the spectral resolution required to give insight into the velocity details and the possible shell structure of the emission regions.

The $J = 6 \rightarrow 5$ emission could have its origin in an even cooler region farther behind such a shock front. In this region, however, the gas velocity has also dropped to substantially below its value at the shock front, and it

We wish to thank C. J. Peruso, C. L. Lowe, T. Kostiuk, and C. D. Parker for support of this experiment. We also acknowledge the leadership of N. McAvoy in the submillimeter laser program during the past several years. The helpful comments of S. G. Kleinmann in preparing this paper are greatly appreciated. Finally, we wish to express our appreciation to E. E. Becklin and the staff of the Mauna Kea IRTF for their enthusiastic support of this experiment.

REFERENCES

Chevalier, R. A. 1980, *Ap. Letters*, **21**, 57.
Erickson, N. R. 1979, Ph.D. thesis, University of California, Berkeley.
Fetterman, H. R., Tannenwald, P. E., Clifton, B. J., Parker, C., Fitzgerald, W. D., and Erickson, N. R. 1978, *Appl. Phys. Letters*, **33**, 151.
Fetterman, H. R., *et al.* 1981, *Science*, **211**, 580.
Goldsmith, P. F., *et al.* 1981, *Ap. J. (Letters)*, **243**, L79.
Goldreich, P., and Kwan, J. 1974, *Ap. J.*, **189**, 441.
Green, S., and Chapman, S. 1978, *Ap. J. Suppl.*, **37**, 167.
Hollenbach, D., and McKee, C. F. 1979, *Ap. J. Suppl.*, **41**, 555.
Hollis, J. M., Snyder, L. E., Buhl, D., and Giguere, P. T. 1975, *Ap. J.*, **200**, 584.
Huggins, P. J., Phillips, T. G., Blair, G. N. and Solomon, P. M. 1981, *Ap. J.*, **244**, 863.
Koepf, G. H., Fetterman, H. R., and McAvoy, N. 1980, *Internat. J. Infrared and Millimeter Waves*, **1**, 597.
Kuiper, T. B. H., Knapp, G. R., Knapp, S. L., and Brown, R. L. 1976, *Ap. J.*, **204**, 408.
Kwan, J. 1977, *Ap. J.*, **216**, 713.
Kwan, J., and Scoville, N. Z. 1976, *Ap. J. (Letters)*, **210**, L39.
Linke, R. A., Goldsmith, P. F. Wannier, P. G., Wilson, R. W., and Penzias, A. A. 1977, *Ap. J.*, **214**, 50.
McKee, C. F. Storey, J. W. V., Watson, D. M., and Green, S. 1982, *Ap. J.*, in press.
Nadeau, D., and Geballe, T. R. 1979, *Ap. J. (Letters)*, **230**, L169.
Phillips, T. G., Huggins, P. J., Neugebauer, G., and Werner, M. W. 1977, *Ap. J. (Letters)*, **217**, L161.
Phillips, T. G., Huggins, P. J., Wannier, P. G., and Scoville, N. Z. 1979, *Ap. J.*, **231**, 720.
Phillips, T. G., Knapp, G. R., Huggins, P. J., Werner, M. W., Wannier, P. G., Neugebauer, G., and Ennis, D. 1981, *Ap. J.*, **245**, 512.
Plambeck, R. L., and Williams, D. R. W. 1979, *Ap. J. (Letters)*, **227**, L43.
Scoville, N. Z., and Solomon, P. M. 1974, *Ap. J. (Letters)*, **187**, L67.
Solomon, P. M., Huguenin, G. R., and Scoville, N. Z., 1981, *Ap. J. (Letters)*, **245**, L19.
Storey, J. W. V., Watson, D. M., Townes, C. H., Haller, E. E., and Hansen, W. L. 1981, *Ap. J.*, **247**, 136.
van Vliet, A. H. F. 1981, Ph.D. thesis, University of Utrecht, Netherlands.
Wannier, P. G., Leighton, R. B., Knapp, G. R., Redman, R. O., Phillips, T. G., and Huggins, P. J. 1979, *Ap. J.*, **230**, 149.
Wannier, P. G., and Phillips, T. G. 1977, *Ap. J.*, **215**, 796.
Watson, D. M., Storey, J. W. V., Townes, C. H., Haller, E. E., and Hauser, W. L. 1980, *Ap. J. (Letters)*, **239**, L129.
Wright, E. L. 1976, *Ap. J.*, **210**, 250.
Zuckerman, B., Kuiper, T. B. H., and Rodriguez Kuiper, E. N. 1976, *Ap. J. (Letters)*, **209**, L137.

G. A. KOEPF: Comsat, Inc., 22300 Comsat Drive, Clarksburg, MD 20871

D. BUHL and G. CHIN: Code 693, NASA/Goddard Space Flight Center, Greenbelt, MD 20771

B. J. CLIFTON, H. R. FETTERMAN, D. D. PECK, and P. E. TANNENWALD: Lincoln Laboratory, Massachusetts Institute of Technology, Lexington, Massachusetts 02173

APPENDIX VI

International Journal of Infrared and Millimeter Waves, Vol. 5, No. 3, 1984

MOLECULAR ASTRONOMY USING HETERODYNE DETECTION AT 691 GHz

D. D. Peck[1] and H. R. Fetterman[2]

Lincoln Laboratory, Massachusetts Institute of Technology
Lexington, Massachusetts 02173

D. Buhl,[1] G. Chin,[1] and S. Petuchowski[1]
NASA/Goddard Spaceflight Center
Greenbelt, Maryland 20771

Received October 3, 1983

Abstract

Observations of the CO J=6→5 transition at 691 GHz (434 μm) in new interstellar and planetary sources have been made. The heterodyne receiver uses an optically pumped laser local oscillator and a quasi-optical Schottky diode mixer, with measured noise temperatures consistently under 4000 K (double sideband). Continued improvements in system performance and antenna coupling have made possible the mapping of 434 μm emission from W3, and the detection of CO J=5→6 absorption in the atmosphere of Venus. A detailed description of the instrumentation and recent observational data are provided.

Key words: submillimeter astronomy, heterodyne radiometry, laser local oscillator, Schottky diode mixer, quasi-optics.

[1]Visiting Astronomer at the Infrared Telescope Facility, which is operated by the University of Hawaii from the National Aeronautics and Space Administration.

[2]Present address: Electrical Sciences and Engineering Department, UCLA.

0195-9271/84/0300-0329$03.50/0 1984 Plenum Publishing Corporation

Introduction

Ground-based astronomy at wavelengths between 100 μm and 1 mm is severely restricted by the opacity of the atmosphere, primarily due to water vapor absorption, and to a lesser extent, other molecular constituents. The recent construction of infrared telescopes at high altitude sites, such as the Infrared Telescope Facility (IRTF) atop Mauna Kea, Hawaii, and Cerro Tololo in Chile, now provide submillimeter astronomers with the opportunity to make extended observations above a substantial fraction of the atmosphere. The advantage of such a site is considerable, but sensitive receivers and protracted integration time are still normally required to achieve adequate signal to noise. A number of innovative techniques have been developed for submillimeter detection, and for the astronomer the choice is generally a compromise among resolution, bandwidth, and sensitivity.

CO, a stable and therefore abundant interstellar molecule, has been identified in scores of astronomical objects. The large dipole moment associated with CO makes it particularly useful as a probe of molecular hydrogen, assuming thermal equilibrium. Several CO rotational transitions have been observed in the molecular cloud Orion, using both coherent and incoherent techniques. This particular object is noted for its breadth, extending more than 30 arcminutes ($\approx 1.5 \times 10^{19}$ cm).[1]

Coherent heterodyne receivers employing InSb hot electron bolometers as detectors/mixers have been used to observe the lower frequency transitions (J=2→1, J=3→2).[2,3] The high resolution intrinsic to heterodyne detection has yielded narrow spectral features that provide important information about the chemistry and kinetics of interstellar gas clouds. The disadvantage of this technique is the limited instantaneous bandwidth (≈ 1 MHz) associated with InSb detectors. Until recently, higher frequency CO transitions have been limited to observation by incoherent detection using passive interferometric filtering for spectral analysis.[4] This method suffers from relatively poor frequency resolution, revealing insufficient information

concerning the physical mechanisms within the astronomical source.

Instrumentation

In an effort to overcome these obstacles, a receiver has been developed that incorporates a stabilized laser local oscillator within a heterodyne radiometer. A block diagram of the receiver is illustrated in Fig. 1.

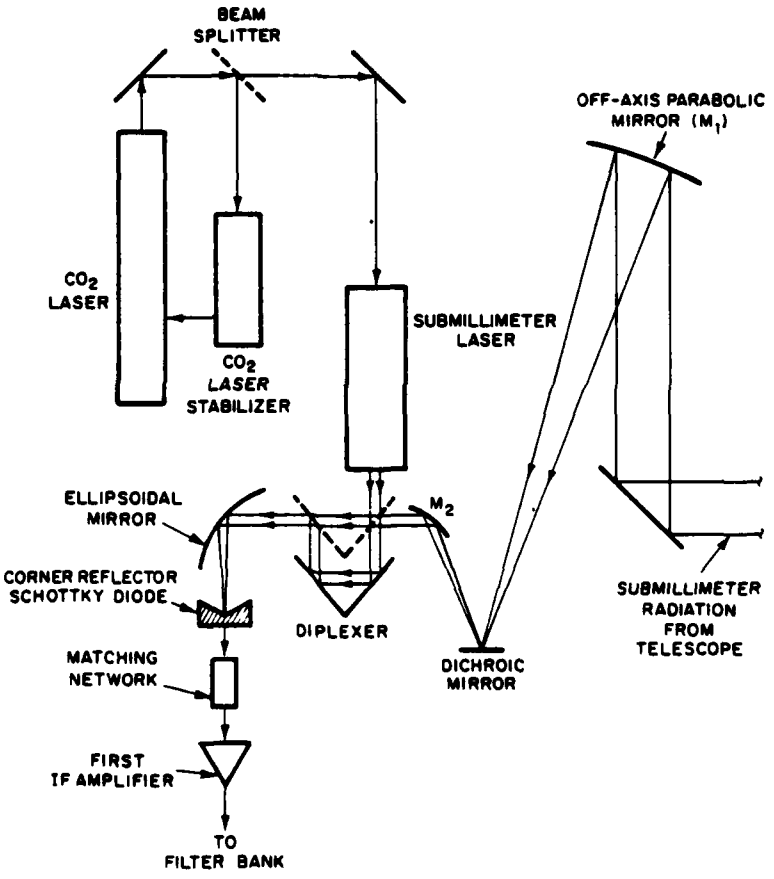

Figure 1. The coherent quasi-optical receiver includes a 692 GHz laser local oscillator.

The development of a quasi-optical Schottky diode mixer mounted in a corner reflector configuration, demonstrating high sensitivity at submillimeter frequencies (NEP = 1.3×10^{-19} W/Hz at 670 GHz), suggested the possibility of astronomical measurements.[5] The 15° FWHM acceptance angle of the mixer permits free-space coupling to the antenna with minimal signal loss. The extremely broad bandwidth (>18 GHz) of these devices is ideally suited for spectral analysis of atmospheric and extraterrestrial molecular transitions, which typically exhibit linewidths of 100 MHz or more because of the large velocity distributions.[6] This characteristic allows the entire spectrum to be acquired simultaneously with a filter bank, an important consideration when fluctuating atmospheric conditions and dynamic sources give rise to time-variant signals. By avoiding the need to retune the local oscillator or filters, acquisition time is determined only by the signal strength of the source.

At present, the requisite power and attainable spectral purity of the local oscillator mandates the use of a laser at frequencies above 300 GHz. Although optically pumped submillimeter lasers do not provide the tunable frequency continuum normally expected of a local oscillator, they have an abundance of discrete far infrared lines that make them quite suitable. The primary disadvantage of using a free-running laser local oscillator is significant frequency and amplitude instability. This instability can be attributed, in part, to thermal expansion of the resonator cavities, resulting in long term drift. Feedback into the CO_2 pump laser, in turn, enhances acoustic noise, creating audio frequency modulation. The lower limits of the radiometer's resolvable bandwidth are defined by such instability. In order to fully exploit the advantages of the receiver, the drift and noise have to be reduced to a minimum. The CW far infrared (FIR) laser designed at NASA/GSFC employed several techniques to improve these characteristics.

Passive stabilization of the FIR cavity was implemented by using invar rods for mirror separation, with aluminum sleeves compensating for the slight thermal expansion of the rods. Active frequency locking of the

CO_2 pump laser was achieved by rotating a ZnSe window in the beam path slightly from Brewsters angle and sampling a small fraction of the beam. This portion was monitored by a temperature-controlled Fabry-Perot cavity, from which an error signal was derived and fed back to a piezoelectric translator controlling the CO_2 laser cavity length. Finally, the CO_2 pump beam was injected into the FIR resonator off-axis. This provided for well-controlled propagation of the pump beam, and eliminated reflections from coupling back into the CO_2 laser. By these means short-term frequency fluctuations were limited to < 10 kHz, and long-term drift was reduced to 14 kHz/min. A complete description of the local oscillator has been given elsewhere.[7]

The J=6→5 transition of CO, the source of emission for these experiments, lies at a rest frequency of 691.47 GHz, on the edge of an atmospheric transmission window. A CHOOH (formic acid) laser, oscillating at 692.95 GHz when pumped by the 9R20 line of the CO_2 laser (45W), was chosen as the local oscillator. This particular laser consistently provided 15 to 20 mW, with outstanding stability characteristics when operated as described above.

Optics

All of the observations performed with the receiver thus far have been made at NASA's Infrared Telescope Facility (IRTF) on the summit of Mauna Kea at an altitude of 4200 m. The telescope has a 3m primary reflector, and uses a computer system capable of tracking targets with < 2 arcsecond pointing accuracy. Since the instrumentation in these experiments was complex and rather unwieldy, the receiver could not be mounted directly on the telescope structure. Instead, the system was placed on an optical table at the coude´ focus of the telescope which provided an f/120 signal beam. In an effort to match the beam with the acceptance angle of the corner-cube mixer, the signal was directed through a series of off-axis parabolic mirrors. The beam, as well as the local oscillator, was coupled to the mixer through an optical diplexer, whose separation was determined by the intermediate frequency of the receiver. By placing a 77 K blackbody load at the subreflector, optical losses

The second experiment benefited from superior observing conditions, with transmission occasionally exceeding 40% at 692 GHz. This excellent atmospheric transparency allowed signal averaging to be reduced to 5 to 10 minutes per spectrum, and permitted the spatial mapping of Orion, as well as the identification of 7 other sources (Fig. 2). The spectral structure observed

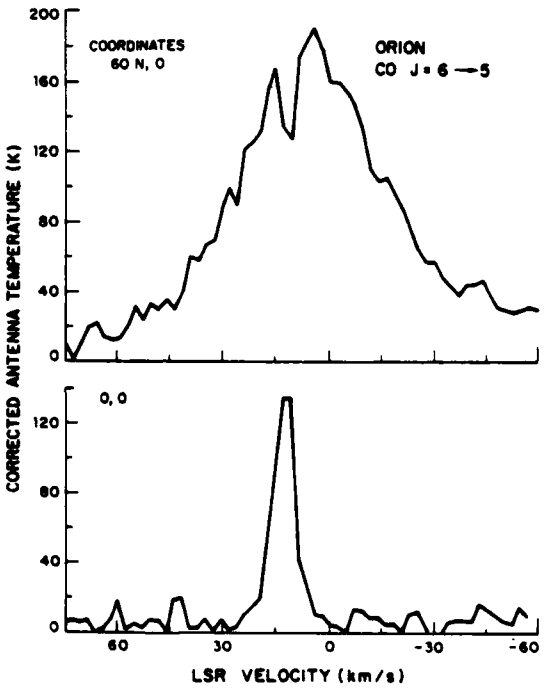

Figure 2. Two spectra observed in the Orion molecular cloud, separated by 1 arcminute. The broad "plateau emission" is believed to be from an optically thin source, while the narrow feature arises in an optically thick region. The frequency information has been transformed into Doppler velocity with respect to the astronomical local standard of reference.

were determined to be about 30% between the telescope and the detector. These losses can be attributed primarily to sidelobes present in the detector antenna pattern. The system noise temperature of the receiver during the most recent observation was as low as 3700 K double sideband.

Signal Processing

The IF signal is directed through a matching network to a low noise (50 K), narrow band (300 MHz) amplifier. Spectral analysis is performed by a 32 channel filter bank using 1 MHz or 5 MHz filters, at the discretion of the observer. A minicomputer is then used to record data, perform signal averaging, and direct the telescope beam switching.

Calibration

In order to accurately calibrate the receiver, signal absorption in the atmosphere had to be determined precisely. The opacity of the atmosphere is highly variable, depending on the amount of precipitable H_2O within the field of view of the telescope. Typical values for water vapor at Mauna Kea range from 0.5 mm to 2.5 mm, corresponding to transmission between 50% and 10% at $\lambda = 434$ μm. The atmospheric transmission was determined before each observing period by evaluating the sky temperature measured at the receiver with the telescope at zenith. The differential increase in sky temperature as the telescope moves away from zenith is then used to calibrate total optical depth.[7] Finally, the continuum emission from a known source, typically Jupiter or Venus, was detected, permitting absolute calibration of antenna temperature.

Results

The initial field test of the receiver successfully detected the presence of emission from the CO J=6→5 transition in the Orion Nebula.[8] Several hours of integration time were required to achieve adequate signal to noise due to high levels of precipitable moisture in the atmosphere. This prevented the examination of other possible sources.

in the map of CO distribution in the J=6→5 transition exhibits some striking variations from similar measurements at lower frequency transitions, although the antenna temperature for the extended emission is in general agreement with predictions made from lower frequency data.[9] Earlier astronomical models used to describe the kinetic processes within Orion must be modified in order to account for the new results. In particular, the source of CO excitation will come under careful scrutiny.

A similar map of the W3 molecular cloud was constructed from data collected during the latest observations (Fig. 3). In contrast to the Orion spectra, these profiles show no evidence of a broad plateau emission. Their appearance is essentially similar to spectra obtained from the J=1→0 transition in the same source.[10] CO J=5→6 absorption in the atmosphere of Venus was also observed for the first time (Fig. 4). The 40 MHz FWHM linewidth is considerably broader than that observed previously in the J=0→1 profiles.[11] This suggests that the J=5→6 absorption occurs at an altitude at least 20 km lower than the J=0→1 transitions. The increased pressure broadening at the lower altitude would account for the linewidth differential. Additional measurements at intermediate transition frequencies will allow a complex model of the atmosphere to be developed. A detailed analysis of the most recent data will be provided in a forthcoming publication.[12]

Conclusions

The success of three consecutive field observations at IRTF has proved the merit of the heterodyne receiver at submillimeter wavelengths. However, the present scale of the instrumentation imposes serious limitations on routine astronomical use. Progress is being made in reducing the physical dimensions of the system through a variety of means. The local oscillator, by far the most massive element, is the focus of particular attention. Relatively simple modifications may result in substantial mass reduction. New designs for the laser will save weight through the substitution of modified structures, using ligher alloys, for passive stabilization. Improved

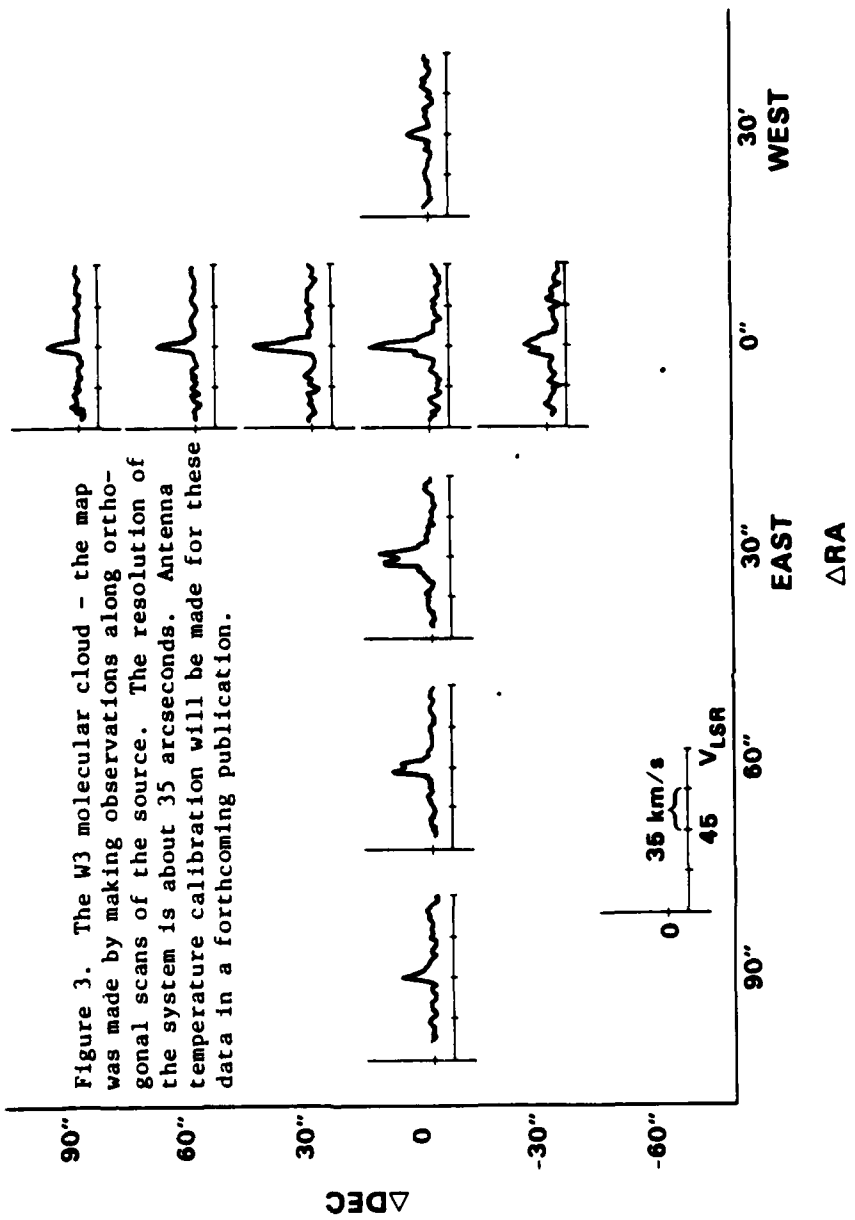

Figure 3. The W3 molecular cloud - the map was made by making observations along orthogonal scans of the source. The resolution of the system is about 35 arcseconds. Antenna temperature calibration will be made for these data in a forthcoming publication.

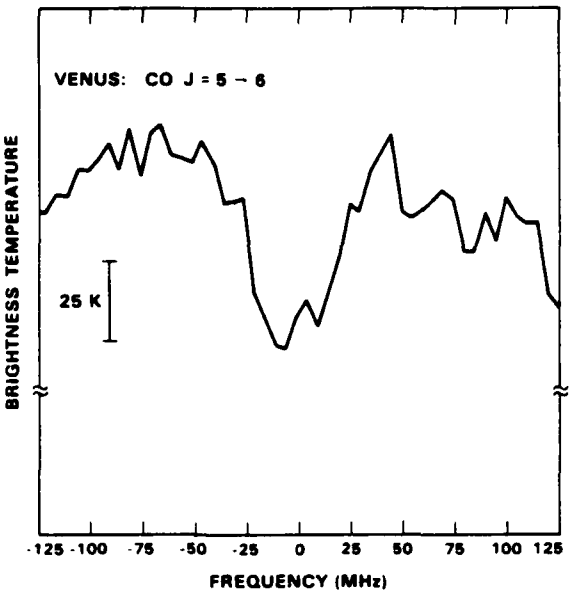

Figure 4. CO J = 5→6 absorption in the atmosphere of Venus. The linewidth is attributed to pressure broadening at lower altitudes.

FIR laser efficiency may reduce the necessary CO_2 pump power and, therefore, the size of the pump laser. Alternative local oscillator sources may soon be available, and will be considered as replacements. These include the use of conventional millimeter wave tube and solid-state sources in conjunction with fundamental waveguide harmonic generators.[13] A crossed-guide harmonic mixer has recently been used as a local oscillator in spectroscopic observations of the 557 GHz ortho-H_2O rotational transition (1_{10}-1_{01}). The mixer was pumped by a carcinotron emitting less than 2 mW at the fundamental frequency of 281.5 GHz.[14] BWO tubes with fundamental frequencies extending into the submillimeter may also prove feasible. An acousto-optic spectrometer has been developed to replace the discrete filter bank. This should result in increased performance (< 1 MHz resolution, > 500 MHz BW), as well as offer considerable savings in size and weight.

A compact receiver using a remote control system capable of monitoring and correcting all critical parameters will be tested in the near future on the cassegrain focus at IRTF. Such a modification will be necessary on a proposed experiment aboard NASA's Kuiper Airborne Observatory, as well as possible future use on an orbiting space telescope.

Acknowledgements

We wish to thank G. A. Koepf, C. J. Peruso, J. Bufton, C. L. Lowe, and C. D. Parker for their invaluable contributions to this experiment. We also express our appreciation to E. E. Becklin and the staff of IRTF for their enthusiastic support.

References

1. H. R. Fetterman, G. A. Koepf, P. F. Goldsmith, B. J. Clifton, D. Buhl, N. R. Erickson, D. D. Peck, N. McAvoy, and P. E. Tannenwald, Science 211, 580 (1981).

2. P. G. Wannier and T. G. Phillips, Astrophys. J. 215, 796 (1977).

3. T. G. Phillips, P. J. Huggins, G. Neugebauer and M. W. Werner, Astrophys. J. 217, L161 (1977).

4. D. M. Watson, J. W. V. Storey, C. H. Townes, E. E. Haller and W. L. Hansen, Astrophys. J. Lett. 239, L129 (1980).

5. H. R. Fetterman, P. E. Tannenwald, B. J. Clifton, C. D. Parker, W. D. Fitzgerald, and N. R. Erickson, Appl. Phys. Lett. 33(2), 151 (1978).

6. R. E. Hills, A. S. Webster, D. A. Alston, P. L. R. Morse, C. C. Zammit, D. H. Martin, D. P. Rice, and E. I. Robson, Infrared Phys. 18, 819 (1978).

7. G. A. Koepf, H. R. Fetterman, and N. McAvoy, Int. J. of IR and MM Waves, 1, 597 (1980).

8. P. F. Goldsmith, N. R. Erickson, H. R. Fetterman, B. J. Clifton, D. D. Peck, P. E. Tannenwald, G. A. Koepf, D. Buhl, and N. McAvoy, Astrophys. J. 243, L79 (1981).

9. G. A. Koepf, D. Buhl, G. Chin, D. D. Peck, H. R. Fetterman, B. J. Clifton, and P. E. Tannenwald, Astrophys. J. 260, 584 (1982).

10. E. Brackmann and N. Scoville, Astrophys. J. 242, 112 (1980).

11. R. K. Kakar, J. W. Waters, and W. J. Wilson, Science 191, 379 (1976).

12. D. Buhl, in preparation (1984).

13. N. R. Erickson and H. R. Fetterman, Bull. Am. Phys. Soc. 27 836 (1982).

14. G. F. Dionne, H. R. Fetterman, N. R. Erickson, C. D. Parker, and J. F. Fitzgerald, Solid S. Res. Rept., Lincoln Laboratory, M.I.T., p. 33 (1982:4); submitted for publication, IEEE J. Quantum Elec.

END

FILMED

9-85

DTIC

REPRODUCED AT GOVERNMENT EXPENSE